A THESIS SUBMITTED TO
THE GRADUATE SCHOOL OF NATURAL AND APPLIED SCIENCES
OF ÇANKIRI KARATEKİN UNIVERSITY

THEORETICAL INVESTIGATION OF SPECTROSCOPIC AND SOME ELECTRONIC PROPERTIES OF (E)-4-((P-TOLYLIMINO) METHYL) PHENYL ACRYLATE SCHIFF BASE BY DFT METHOD

IN PARTIAL FULFILLMENT OF THE REQUIREMENTS
FOR
THE DEGREE OF MASTER OF SCIENCE
IN
PHYSICS

BY

ABDULRAHMAN JAMAL HASHIM AL-DHUWAIB

ÇANKIRI

2023

THEORETICAL INVESTIGATION OF SPECTROSCOPIC AND SOME ELECTRONIC PROPERTIES OF (E)-4-((P-TOLYLIMINO)METHYL)PHENYL ACRYLATE SCHIFF BASE BY DFT METHOD

By Abdulrahman Jamal Hashım AL-DHUWAIB

May 2023

We certify that we have read this thesis and that in our opinion it is fully adequate, in scope and in quality, as a thesis for the degree of Master of Science

Advisor **:** Prof. Dr. Hamit ALYAR

Examining Committee Members:

Chairman **:** Prof. Dr. Mustafa Kemal ÖZTÜRK
Physics
Gazi University

Member **:** Prof. Dr. Hamit ALYAR
Physics
Çankırı Karatekin University

Member **:** Prof. Dr. İlyas İNCİ
Physics
Çankırı Karatekin University

Approved for the Graduate School of Natural and Applied Sciences

Prof. Dr. HAMİT ALYAR
Director of Graduate School

I hereby declare that all information in this document has been obtained and presented in accordance with academic rules and ethical conduct. I also declare that, as required by these rules and conduct, I have fully cited and referenced all material and results that are not original to this work.

Abdulrahman Jamal Hashım AL-DHUWAIB

ABSTRACT

THEORETICAL INVESTIGATION OF SPECTROSCOPIC AND SOME ELECTRONIC PROPERTIES OF (E)-4-((P-TOLYLIMINO) METHYL) PHENYL ACRYLATE SCHIFF BASE BY DFT METHOD COMPOUND

Abdulrahman Jamal Hashım AL-DHUWAIB

Master of Science in Physics

Advisor: Prof. Dr. Hamit ALYAR

May 2023

Schiff bases; They are compounds that have importance in various branches such as pharmacy, medicine, biological systems, cosmetics, agriculture, production of dyes, plastics industry, aircraft industry, liquid crystal technology, electronics industry and analytical chemistry.

The present study aims to theoretically investigate the spectroscopic and electronic properties of (E)-4-((P-tolylimino) methyl) phenyl acrylate Schiff base using the Density Functional Theory (DFT) method. The structure of Schiff base molecule was theoretically elucidated by FT-IR and NMR spectroscopy. The molecular geometry of the Schiff base was drawn with the Gauss View 5.0 program and its structure was optimized using the B3LYP/6-311++G(d,p) theory level DFT method. After the optimization calculation, the harmonic frequency calculation was made and it was understood that the molecule was in a stable structure since no negative frequency was observed as a result of the calculation. Since the studied Schiff base does not have crystal data in the literature, it was compared with the structural parameters of similar molecules and it was seen that the results were compatible with the experimental data. The vibration frequencies were marked and it was seen that the calculated theoretical frequency values were in good agreement with the experimental spectra. The calculated NMR chemical shifts were also found to be in good agreement with the experimental values. Also, nonlinear optical (NLO) properties of Schiff base with HOMO-LUMO molecular orbital energies were

calculated and found to have significant NLO activity. Finally, the molecular electrostatic potential (MEP) analysis was performed to study the reactivity and potential sites of electrophilic and nucleophilic attacks. The results of this study provide valuable insights into the spectroscopic and electronic properties of the (E)-4-((P-tolylimino) methyl) phenyl acrylate Schiff base and could be useful in designing novel organic materials with promising optical and electronic properties.

2023, 55 pages

Keywords: Schiff base, FT-IR, NMR, NLO, DFT

ÖZET

(E)-4-((P-TOLILIMINO)METIL)FENIL AKRILAT SCHIFF BAZININ SPEKTROSKOPIK VE BAZI ELEKTRONIK ÖZELLIKLERININ TEORIK OLARAK INCELENMESI

Abdulrahman Jamal Hashım AL-DHUWAIB
Fizik, Yüksek Lisans
Tez Danışmanı: Prof. Dr. Hamit ALYAR
May 2023

Schiff bazları; eczacılıkta, tıpta, biyolojik sistemlerde, kozmetikte, tarım alanında, boyar maddelerin üretiminde, plastik sanayisinde, uçak sanayisinde, sıvı kristal teknolojisinde, elektronik endüstrisinde ve analitik kimya gibi çeşitli dallarda öneme sahip bileşiklerdir. Bu çalışma, Yoğunluk Fonksiyonel Teorisi (DFT) yöntemini kullanarak (E)-4-((P-tolilimino)metil) fenil akrilat Schiff bazının spektroskopik ve elektronik özelliklerini teorik olarak araştırmayı amaçlamaktadır. Schiff bazı molekülünün yapısı FT-IR ve NMR spektroskopisi ile teorik olarak aydınlatıldı. Schiff bazının moleküler geometrisi Gauss View 5.0 programıyla çizildi ve yapısı B3LYP/6-311++G(d,p) teori düzeyinde DFT metodu kullanılarak optimize edildi. Optimizasyon hesabından sonra harmonik frekans hesabı yapıldı ve hesaplama sonucunda negatif frekans görülmediği için molekülün kararlı yapıda olduğu anlaşıldı. Çalışılan Schiff bazının literatürde kristal verileri olmadığı için benzer moleküllerin yapısal parametreleri ile karşılaştırılması yapıldı ve deneysel verilerle uyumlu sonuçlar elde edildiği görüldü. Titreşim frekanslarının işaretlemeleri yapıldı ve hesaplanan teorik frekans değerlerinin deneysel spektrumlarla iyi bir uyum içinde olduğu görüldü. Hesaplanan NMR kimyasal kaymalarının da deneysel değerlerle iyi bir uyum içinde olduğu bulundu. Ayrıca, Schiff bazının HOMO-LUMO moleküler orbital enerjileri ile doğrusal olmayan optik (NLO) özellikleri hesaplandı ve önemli ölçüde NLO aktivitesine sahip olduğu bulundu. Son olarak, elektrofilik ve nükleofilik saldırıların reaktivitesini ve potansiyel bölgelerini incelemek için moleküler elektrostatik potansiyel (MEP) analizi yapıldı. Bu çalışmanın sonuçları, (E)-4-((P-tolilimino)metil) fenil akrilat Schiff bazının spektroskopik ve elektronik özelliklerine

ilişkin değerli bilgiler sağlar ve gelecek vaat eden optik ve elektronik özelliklere sahip yeni organik materyallerin tasarlanmasında faydalı olabilir.

2023, 55 sayfa

Anahtar Kelimeler: Schiff bazı, FT-IR, NMR, NLO, DFT

PREFACE AND ACKNOWLEDGEMENTS

Praise is to Allah, whose grace is done good deeds. I would like to thank my thesis advisor Prof. Dr. Hamit Alyar for guiding me in my dissertation and for his direct supervision, patience and understanding. I dedicate this work to Prof. Dr. Hamit Alyar, who was credited with completing it after Allah Almighty. I do not forget my father and mother who supported me with everything possible, as well as my wife who supported me in my new period in life, my brothers, my friend Hassanein Abdulkarim, Dr.Abdullah Nafea and all my loved ones and those who helped me.

Abdulrahman Jamal Hashım AL-DHUWAIB
Çankırı-2023

CONTENTS

ABSTRACT ..... **i**
ÖZET ..... **iii**
PREFACE AND ACKNOWLEDGEMENTS ..... **v**
CONTENTS ..... **vi**
LIST OF SYMBOLS ..... **viii**
LIST OF ABBREVIATIONS ..... **ix**
LIST OF FIGURES ..... **x**
LIST OF TABLES ..... **xi**
1. INTRODUCTION **1**
2. LITERATURE REVIEW **3**
2.1 Electromagnetic Waves **3**
2.1.1 Radio waves **4**
2.1.2 Microwaves **5**
2.1.3 Infrared Waves(IR) **5**
2.1.4 Visible rays **6**
2.1.5 Ultraviolet rays (UV) **6**
2.1.6 X-ray **6**
2.1.7 Gamma ray (γ) **7**
2.2 Spectroscopy **7**
2.3 Spectroscopic Methods **7**
2.3.1 UV-Visible absorbtion spectroscopy **7**
2.3.2 Atomic Absorbtion spectroscoy **8**
2.3.3 Nuclear Magnetic Resonance spectroscoy **9**
2.3.4 Mass spectroscoy **10**
2.3.5 X-ray spectroscoy **11**
2.3.6 Gamma ray spectroscoy **12**
2.3.7 Raman spectroscoy **12**
2.3.8 Infrared spectroscoy **13**
2.4 Molecular Vibration Types **14**
2.4.1 Stretching vibrations(v) **14**

2.4.2 Bending vibrations(σ) 14
2.4.3 Torsion vibrations(τ) 15
2.5 Molecular Modeling With Quantum Mechanical Methods 16
2.5.1 Quantum mechanics equation of motion: Schrödinger equation 16
2.5.2 Born - Oppenheimer approach 17
2.5.3 Slater determinant 18
2.6 Molecular Modeling Methods 19
2.6.1 Molecular mechanical method 19
2.6.2 Semi empirical method 20
2.6.3 Ab Initio method 21
2.6.4 Hartree - Fock method self-consistent field (SCF) theory 24
2.6.5 Density functional method 25
2.7 Properties Energy Surface 26
2.8 Geometry Optimization 27
2.9 Slater Type Orbitals 28
2.10 Gaussian Type Orbitals 28
2.11 Basis Sets 29
3. MATERIALS AND METHODS 31
4. RESULTS AND DISCUSSION 32
4.1 Geometrical Optimization of the (E)-4-((p-tolylimino)methyl)phenyl acrylate compound ……32
4.2 Vibrational Assignment of (E)-4-((p-tolylimino)methyl)phenyl acrylate compound 35
4.3 NMR Results of (E)-4-((p-tolylimino)methyl)phenyl acrylate compound 38
4.4 HOMO-LUMO Analyze 40
4.5 Nonlinear Optical (NLO) Properties 41
4.6 Molecular Electrostatic Potential (MESP) 44
5. CONCLUSIONS AND RECOMMENDATION 45
REFERENCES 47
CURRICULUM VITAE 55

LIST OF SYMBOLS

δ	Bending vibrations
S_{ik}	Covering integral
H_{ik}	Hamiltonian matrix
$\hat{H}$	Hamiltonian processor
β_{tot}	Hyperpolarizability
β	In-plane angle bending
$\hat{T}$	Kinetic energy
γ	Out -of-plane angle bending
α_{ave}	Polarizability
ν	Stress vibrations
τ	Torsion vibration
Ψ	Wave function
ε_r	Dielectric constant
μ_o	The permeability of free space or vacuum
C	Speed of light
h	Planck constant
K	Wavenumber
t	Twisting
α_{ave}	Polarizability
δs	Scissoring
E	Energy eigen value
ε_0	The permittivity of free space or vacuum
λ	Wavelengith
ν_{as}	Asymmetric stretching
ν_s	Symmetric stretching
P	Total electron density
σi	Spin coordinate
ω	Wagging vibration
ν	Stretching vibrations
ρ	Rocking vibration
∇_i^2	Laplacian operator

LIST OF ABBREVIATIONS

AAS	Atomic bbsorption spectroscopy
BO	……Born-Oppenheimer
DFT	Density functional theory
FT-IR	Fourier-transform infrared spectroscopy
GTOs	Gaussian type orbitals
HOMO	Highest occupied molecular orbital
LUMO	Lowest unoccupied molecular orbital
MEP	Molecular electrostatic potential
MS	……Mass spectrometry
NLO	Nonlinear optic
PES	Potential energy surface
SCF	Self-consistent field
STO	Slater type orbitals

LIST OF FIGURES

Figure 1.1 General representation of Schiff bases 1
Figure 2.1 The various parts of the electromagnetic spectrum (Baden Fuller 1979) 4
Figure 2.2 The basic components of a mass spectrometer (Khopkar 1998) 11
Figure 2.3 The types of stretching vibration (Skoog and Leary 1992) 14
Figure 2.4 Bending vibrations (Ojeda and Dittrich 2012) 15
Figure 2.5 Dihedral angle definition (Coates 2006) 15
Figure 4.1 Optimized structure of the compound 32
Figure 4.2 FT-IR spectrum of (E)-4-((p-tolylimino) methyl) phenyl acrylate compound 35
Figure 4.3 ^{1}H-NMR spectrum of (E)-4-((p-tolylimino) methyl) phenyl acrylate compound 39
Figure 4.4 Energy levels and the 3D plots of the HOMO and LUMO (E)-4-((p-tolylimino) methyl) phenyl acrylate compound 41
Figure 4.5 MESP map of (E)-4-((p-tolylimino) methyl) phenyl acrylate compound 44

LIST OF TABLES

Table 4.1 Molecular geometric parameters (bond lengths, bond angles and torsion angles) of (E)-4-((p-tolylimino) methyl) phenyl acrylate compound 33
Table 4.2 Theoretical and experimental(FT-IR)vibration frequencies of the (E)-4-((p-tolylimino) methyl) phenyl acrylate 36
Table 4.3 ^{1}H-NMR and ^{13}C-NMR of (E)-4-((p-tolylimino) methyl) phenyl acrylate compound 39
Table 4.4 The electric dipole moment μ (D), the mean polarizability <α> and the first hyperpolarizability (βtot) of (E)-4-((p-tolylimino)methyl)phenyl acrylate by DFT/B3LYP/6-311++G(d,p) level of theory 43

1. INTRODUCTION

Since a scientist named Schiff first created them in 1864, compounds with the (-C=N-) group in their structure are referred to as "Schiff Bases" (Schiff 1869). The generic formula RCH=NR′, where R and R′ in the formula signify aryl or alkyl substituents, is used to describe Schiff bases (Fig. 1.1).

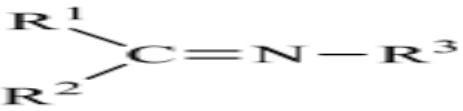

Figure 1.1 General representation of Schiff bases. R1, R2, R3 = aryl or alkyl

Depending on the amount of donor atoms in their structure, Schiff bases can function as polydentate ligands. By giving the metal electron pairs on the nitrogen atoms they contain, they can create complexes. The stability of the cyclic complexes formed by the azomethine groups is increased by the transport of other functional groups (like hydroxyl) that contain displaceable hydrogen atoms adjacent to the azomethine groups.

The bond created by a reaction with an aldehyde is known as an azomethine or an aldimine, whereas the bond created by a reaction with a ketone is known as an imine or a ketamine. Because they are stable and simple to synthesize, Schiff bases (imines) have succeeded in being among the compounds of interest. Imines' employment in numerous biological systems (Sharaby *et al.* 2017), chemical catalysis (Redshaw 2017), medicine and pharmacy (Roberts *et al.* 2017), chemical analyses, and new technologies (Dirisio *et al.* 2017, Upadhyay *et al.* 2008), among other applications, can be used to explain this interest in them.

Coordination chemicals are becoming more and more significant in both biological systems and the industry. Schiff bases are among the ligands widely used in coordination chemistry because of their biological and structural characteristics.

Metal complexes of Schiff bases, whose use as ligands was initially described by Pfeiffer in 1933 (Pfeiffer *et al.* 1933, Seçkin *et al.* 2003), are being researched with interest.

According to (Ashraf et al. 2011), metal-imine complexes have been extensively studied for their potential as herbicides and anticancer agents. According to reports (Ozaslan *et al.* 2011), they have a protective impact on the hematopoietic system. They are also thought of as antibacterial and antifungal agents in addition to their usage as antivirals. (Redshaw 2017, Roberts *et al.* 2017, DiRisio *et al.* 2017, Upadhyay *et al.* 2008, Sharaby *et al.* 2017).

Diabetes and AIDS are also treated with it (Golcu *et al.* 2005, Silva *et al.* 2011, and Rehman *et al.* 2004). Additionally, Schiff bases are employed in a variety of industries, including the paint industry (Serin and Gök 1988), cation carrier, and ion selective electrode production (Aydınlı 2006), corrosion inhibitor (Emregul *et al.* 2006).

The thesis here says, we studied spectroscopic, electronic and nonlinear optical features of (E)-4-((P-tolylimino) methyl) phenyl acrylate. We utilised the 6-311++G (d,p) basis set and the Gaussian 09 program to accomplish all computations.

2. LITERATURE REVIEW

2.1 Electromagnetic Waves

The Latin origin of the word spectrum is "form" or "appearance." The words "species" and "spectacle," which share the same root, are other well-known nouns. In order to describe the rainbow-like pattern that appeared when a sunlight beam traveled through a glass prism, Newton invented the phrase. The many different types of electromagnetic radiation that are categorized today by their frequency or wavelength on a scale from large to tiny are referred to as the electromagnetic spectrum (Sander and Reed 1978).

The only electromagnetic waves that were familiar at the time Maxwell made his prediction about their existence were the visible light waves. It was only recently discovered that ultraviolet and infrared waves exist. The discovery of Gamma rays and X-rays came around the end of the nineteenth century. As of now, we are aware that electromagnetic waves also include UV, infrared, X-ray, gamma, radio, and microwave waves.

The electromagnetic spectrum is a way to categorize electromagnetic waves based on their frequency (Fig.2.1). The line separating one type of wave from the next is not particularly clear. The waves' generation and/or detection processes serve as the basis for the classification (Baden Fuller 1979). In order of decreasing wavelengths, we provide a brief description of these several electromagnetic wave types.

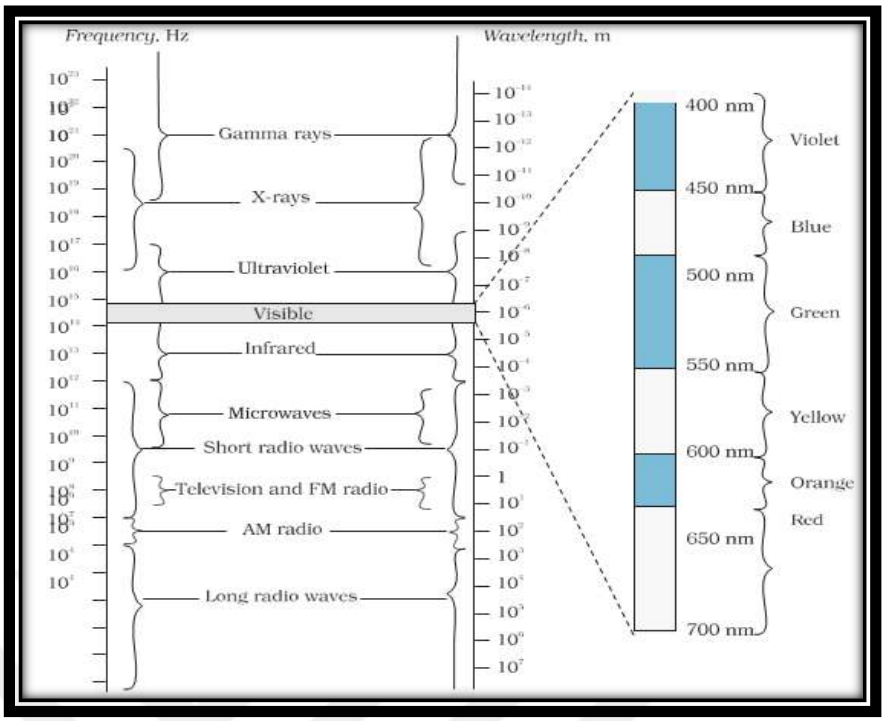

Figure 2.1 The various parts of the electromagnetic spectrum (Baden Fuller 1979).

2.1.1 Radio waves

Accelerated charge mobility radio waves are produced in conducting wires. Systems for radio and television communications, they are employed. They typically operate in the 500 kHz to 1000 MHz frequency band. The AM band spans the range of 530 kHz to 1710 kHz. Higher frequencies up to 54 MHz for short wave bands are employed. The frequency range for TV waves is 54 to 890 MHz the FM (frequency modulated) ranges from 88 MHz to 108 MHz radio band's circumference. The ultrahigh frequency (UHF) band is used by cellular phones to deliver voice communication using radio waves (Ramo *et al.* 1967).

2.1.2 Microwaves

Specialized vacuum tubes generate Short-wavelength radio waves with frequencies in the gigahertz (GHz) region are known as microwaves (called klystrons, magnetrons and Gunn diodes). For the radar systems used in aviation navigation, they are helpful because of their short wavelengths. The timers for fastballs, tennis serves, and automobiles are called speed guns likewise based on radar technology. An intriguing residential use of these waves is microwave units. The frequency of the microwaves in these ovens is chosen to coincide with the resonant frequency of water molecules in order to effectively convert wave energy into molecular kinetic energy. Any food containing water becomes hotter as a result (Cullen 1965).

2.1.3 Infrared-waves

A hot body and chemicals emit IR radiation. This group is located close to the visible spectrum's low-frequency or long-wave length end. Heat waves are another name for infrared waves. Due to the following that most materials include liquid molecule, which easily take in infrared wavelengths (Numerous other chemicals, such CO2 and NH3, also absorb infrared radiation. Their increased thermal mobility after absorption, which causes them to warm up and warm their surroundings. Physical treatment employs the use of infrared lamps. Through the greenhouse effect, infrared radiation also contributes significantly to maintaining the warmth or average temperature of the earth. Visible light strikes the surface of the earth and is absorbed, which travels through the atmosphere quite quickly, and re-radiates it as infrared radiations (longer wavelengths) (Kuhn 1946).

2.1.4 Visible rays

It is the electromagnetic wave type that is most well-known. The area of the spectrum that the human eye can perceive is known as this zone. It has a wavelength range of roughly 700-400 nm and oscillates between 4 and 7×10^{14} Hz. The visible light that is emitted or reflected from the surroundings gives us knowledge of the environment. These wavelengths can be seen by our eyes. Animals vary in their sensitivity to various wavelength ranges. Snakes, for instance, can perceive infrared radiation, and many insects' "visible" ranges extend well into the ultraviolet (Staniforth 1972).

2.1.5 Ultraviolet rays (UV)

It spans wavelengths between 400 nm, or about 4×10^{-7} m, and (6×10^{-10}) m (0.6 nm). The production of UV (ultraviolet) light occurs in specific lamps and extremely heated bodies. A significant source of UV light is the sun. Fortunately, the ozone layer is where most of it is trapped. Which is located in the environment at a height of 40 to 50 km. When UV rays is present in depth doses, it is damaging to people. The skin tans as a result of increased melanin production brought on by UV light exposure. Ordinary glass absorbs UV rays. As a result, it is impossible to burn or tan through glass windows (Cheng 1990).

2.1.6 X-rays

The X-ray portion of the range of electromagnetic waves is located beyond the UV area. Because of their widespread use, we are all familiar with X-rays usage in medicine. It covers wavelengths between approximately 10^{-8} m (10 nm) to 10^{-13} m (10^{-4} nm). High energy electrons are frequently used to attack a metal target in order to produce X-rays. In medicine, X-rays are utilized as a diagnostic tool

as well as a therapy for some forms of cancer. X-rays can cause injury or death to live tissues and creatures. Thus, it is important to minimize exposure that is not necessary or excessive (Collin 1966).

2.1.7 Gamma rays (γ)

They have wavelengths ranging from roughly 10^{-10} meters to less than 10^{-14} meters and are located in the higher frequency band of the electromagnetic radiation spectrum. Both radioactive nuclei and nuclear processes result in the production of this high frequency radiation. In medicine, they are employed to eliminate cancer cells (Benson 1969).

2.2 Spectroscopy

Numerous methods that use radiation to learn about the composition and characteristics of matter collectively fall under the umbrella name "spectroscopy." The fundamental idea behind all spectroscopic approaches is to shine an electromagnetic beam upon a sample and see how it reacts to the stimulation. Typically, the response is quantified as a function of radiation wavelength. A spectrum is a diagram that represents the response as a function of wavelength (Lakowicz 2006).

2.3 Spectroscopy Methods

2.3.1 UV – Visible absorption spectrophotometer

Many molecules absorb ultraviolet or visible light. The most essential absorption process is basic absorption, which includes electrons transitioning from the valance to the conduction spectrum (Hussien Al- kaissy 2011). The beam's intensity, denoted as I_o, must

match the total of the transmitted, absorbed, and reflected beam intensities, which are as shown by I_T, I_A, and I_R, accordingly (William 2003).

$$I_o = I_T + I_A + I_R \quad (2.1)$$

$$T + A + R = 1 \quad (2.2)$$

The absorption is connected to the electronic transition between the V.B. and the C.B., which is dependent on photon energy (hυ), where (h) is Plank's constant and (υ) is incoming photon frequency (Khalaf 2013). If the incident photon's energy (h) is greater than or equal to the photon will interact with the valence electron, raising it into the C.B. and forming an electron-hole pair across the energy gap (Eg). The electron-hole pair's incident photon's maximal wavelength (λ_c) is specified as (Khalaf 2013).

$$\lambda_c = \frac{hc}{E_g} = \frac{1.24}{E_{g(eV)}} \quad (2.3)$$

According to Beer's law, the intensity of the photon flow diminishes exponential with distance through the substance (Meyer 1992).

$$I = I_o e^{-\alpha t} \quad (2.4)$$

Where (I_o, I) are the incident and transmitted photon intensities, and (α) is the absorption coefficient specified in Eq.(2-7), This is defined as the amount of photons absorbed per unit distance of semiconductor, and (t) is the sample thickness (Meyer 1992).

$$\alpha = 2.303 \frac{A}{t} \quad (2.5)$$

Where,(A) is the absorption.

2.3.2 Atomic absorption spectroscopy

Atomic Induction By detecting the radiation that the chemical element of interest absorbs, the spectrometry (AAS) approach may be used to ascertain the amounts of chemical elements that can be found in environmental samples. This is accomplished by analyzing the spectra that are created when radiation excites the material. When ultraviolet or visible light is absorbed, the atoms shift to higher energy levels. The quantity of energy in the form of light photons that are absorbed by the sample is measured by atomic absorption techniques. A detector monitors the light wavelengths that the sample transmits and compares them to the light wavelengths that initially passed through the sample. The

readout's peaks of energy absorption at distinct wavelengths are caused by variations in the wavelength that have been absorbed, which are subsequently integrated by a signal processor. Each chemical element has its unique ionization energy, which is needed for an electron to leave an atom. A photon with energy E is released when an electron in the atom transitions from one energy level to another. An element's atoms emit a distinctive spectral line. Due to the particular arrangement of electrons in each atom's outer shell, each atom has a unique pattern of wavelengths at which it will absorb energy. This makes it possible to analyze a sample's quality. The Beer-Lambert law is used to compute the concentration (García and Báez 2012).

2.3.3 Nuclear magnetic resonance (NMR) spectroscopy

In the last 50 years, nuclear magnetic resonance spectroscopy, or NMR, as a result of the method of preference for figuring out the structure of organic compounds. It is the only spectroscopic method for which a detailed examination and interpretation of the complete spectrum is normally anticipated. NMR is non-destructive, and excellent data may be obtained from materials weighing less than a milligram using contemporary equipment. Even though larger sample quantities are required than for mass spectroscopy (Jaber 2015).

Understanding the underlying physical principles of the methodologies is essential for effective use of (NMR) as an analytical tool. Numerous elemental isotopes have distinctive spins in their nuclei (I). Some nuclei (I = 1, 2, 3, etc.) have integral spins, whereas others (I = 1/2, 3/2, 5/2, etc.) have fractional spins, and a few (I = 0) have no spin (e.g. 12C, 16O, 32S ...). For organic chemists, the isotopes 1H, 13C, 19F, and 31P, that has all I = 1/2, are of great interest and application. Our study NMR will be confined to these and other applications I = 1/2 nuclei since the analysis of this spin state is fairly simple (Rekha and Ramalingam 2009). The NMR phenomenon is caused by the following characteristics (Rekha and Ramalingam 2009).

1. A magnetic field is produced by a rotating charge. (μ) A magnetic moment proportionates to the spin results in a spin magnet.

2- The spin states +1/2 and -1/2 occur when an external magnetic field is present (B_0). The greater energy's magnetic moment -1/2 spin state is in opposition to the outside world, whereas that of the lower energy +1/2 state is aligned with it.
3- The energy differential is affected by the intensity of the external magnetic field.
4- For nuclei with at a given magnetic field intensity, the energy difference between the two spin states will be inversely proportional to spin ½ correlated with their magnetic moments.

The magnetic moments are as follows for the four commonly occurring nuclei mentioned above: 1H μ= 2.7927, 19F μ= 2.6273, 31P μ= 1.1305, and 13C μ= 0.7022. These moments can be detected in nuclear magnetons $5.05078*10^{-27}$ JT^{-1} (Mahdi 2010).

2.3.4 Mass spectroscopy

A complex instrumental technique called mass spectrometry creates, Separates and locates ions in the gas phase. Figure 2.2 illustrates the essential parts of a mass spectrophotometer. Through some sort of input system, samples are fed into the ionization source. Different ionization sources will produce ions in a way that is more or less optimal depends on the analytes' type, phase, and sample. The majority of analyte molecules are neutral; hence they must be ionized. There are numerous ways to do this. High-energies sources such as a discharge of electricity, a laser, or electron bombardment can be used to subject analytes. There are also sources of ionization with lower energy or that are "softer," like those seen in atmospheric pressure ionization (Khopkar 1998).

In the sections below, we give an overview of typical ionization sources. Ions can be produced or quickly moved into a low-pressure (10^{-4} to 10^{-7} Torr) environment where using electric field separation, they may be separated based on their mass-to-charge (m/z) ratio and magnetic fields in a variety of ways. The benefits, drawbacks, prices, and uses of various mass analyzers vary. The separated ions are constructed to affect a detector after that transforms them into electrical signals that may be interpreted a database system There are many different types of detectors, although some like the electron multiplier—are used more frequently than others (Skoog *et al.* 2013).

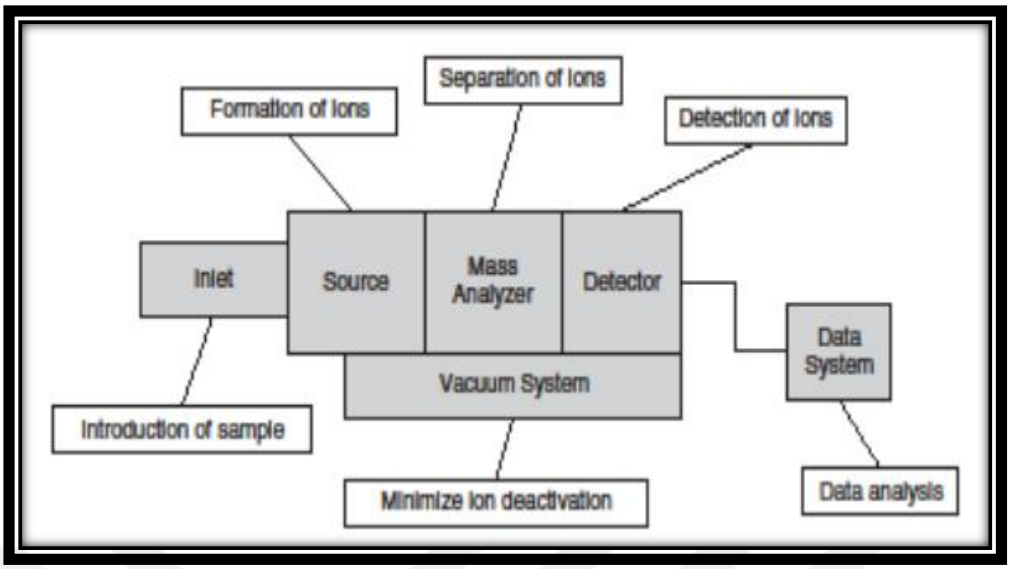

Figure 2.2 The basic components of a mass spectrometer (Khopkar 1998)

2.3.5 X-Ray spectroscopy

A strong method for determining X-ray diffraction reveals the crystal shape and lattice properties (XRD) (Al-Hamdani 2016). The Bragg spectrometer is a fundamental tool for such research (Kiran *et al.* 2010). Bragg's law, which describes the relationship between William H. Bragg and W. Lawrence Bragg, discovered the angle at which a crystal's surface diffracts an X-ray beam of a particular wavelength (Radhi 2012).

$$2d_{(hkl)}\sin\theta = m\lambda \qquad (2.6)$$

Where, (λ) is wavelength of the X-Ray, (θ) is Bragg diffraction angle of the XRD peak in degree (scattering angle), (m) is an integer indicating the diffraction peak's order, and $(d_{(hkl)})$ is the distance between atoms, ions, or molecules. Using Debye Scherrer's formula, the deposits' crystallite size is calculated from the full width at half maximum (FWHM) of the strongest diffraction line (Al-Sarraji 2014).

$$D_S = \frac{0.94\,\lambda}{D\cos\theta} \qquad (2.7)$$

Where, D_S is crystallite size, and in radians, which D is (FWHM). The dimension of the unit cell may also be determined using the X-Ray diffract data.

2.3.6 Gamma ray spectroscopy

The physical basis for gamma spectrometry is the interaction of the target material with gamma rays. Through the electronic components, the signals are received and converted to quantifiable and recordable electric pulse impulses in the gamma spectrometry process. A multi-channel pulse analyzer allows for the nuclide's type may be determined based the concentration might depend on the energy of the electrical pulse peak. Determined by counting the pulses' intensities (Gilmore 2008). The two types of gamma spectrometry are based on the ground and the air on the item being measured (Rouze *et al.* 2017), and the technique is frequently employed in domains such as environmental radiation monitoring, mining radioactive minerals, radiation treatment, and food safety inspections, among other things (Cresswell *et al.* 2018, Khan *et al.* 2010).

2.3.7 Raman-spectroscopy

Spectroscopy using Raman is a method with a focus on determining the frequency shift of inelastic scattered light from the sample when an incident light photon interacts with a molecule to produce a scattered photon (Long 1977). When the frequency of the dispersed light differs from the original frequency, it is said to have undergone Stokes Raman scattering; when it has undergone anti-Stokes Raman scattering. In the latter scenario, when the molecule's bond is originally in the excited vibrational state, the photon will obtain energy from the bond (Kudelski 2009, Kudelski 2008). Raman is often based on measuring the change in energy of the departing photon. The chemical makeup of the molecules that cause scattering determines the shift in light's wavelength that is scattered. The magnitude of the change in the molecule polarization directly relates to the Raman scattering's intensity.

The use of optical fibers in Raman spectroscopy gives remote sensing a significant advantage. By gathering the dispersed photons, the optical fibers are in charge of carrying the Raman signals. The fiber optic system consists of fibers in which the scattered radiations are transferred to the detector along various fibers while the laser excitation is transmitted along a single fiber. Real-time monitoring systems using Raman spectroscopy have been utilized to find illegal substances, environmentally hazardous materials, and chemical and biological warfare agents (Raman and Krishnan 1928).

2.3.8 Infrared (IR) spectroscopy

By measuring the wavelength and intensity of an object's infrared wave absorption, IR spectroscopy is used. The unique twisting, bending, rotating, and vibrational motions of atoms within a molecule are what cause infrared spectra to be produced (Muncheryan 1983). Two categories of molecular vibrations can be used to characterize all of the motions. Bond length changes as a result of one kind of vibration, the stretch. A stretch is an irregular movement made along the atoms' boundary. A change in bond angle is caused by the bend Sound kind of vibration. Stretches can either be symmetrical or asymmetrical. Bending can take place in the molecule's plane or out of it (Lide 2012).

2.4 Molecular vibration types

Stretching or bending is one of the three basic types of molecular vibrations and torsion.

2.4.1 Stretching vibrations (v)

The inter-atomic distance along the bond axis changes as a result of the stretching vibration. Figure (2.3) illustrates the symmetric and asymmetric stretching vibrations, respectively (Skoog and Leary 1992).

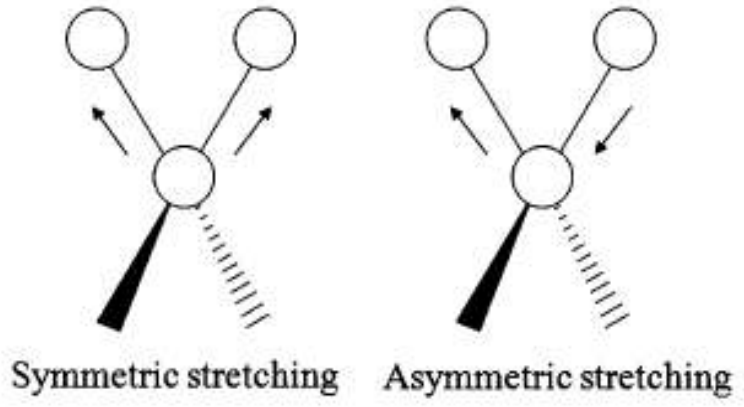

Figure 2.3 The types of stretching vibration (Skoog and Leary 1992).

2.4.2 Bending vibration (σ)

In contrast, the bond angles while bending, bond lengths stay constant while vibrations fluctuate fixed. The four different kinds of bending vibrations are depicted in figure (2.4) (Ojeda and Dittrich 2012) as rocking, scissoring, wagging, and twisting. In the infrared spectrum, stretching absorptions often result in sharper peaks than bending ones; however bending absorptions can be helpful in distinguishing between bonds of the same kind.

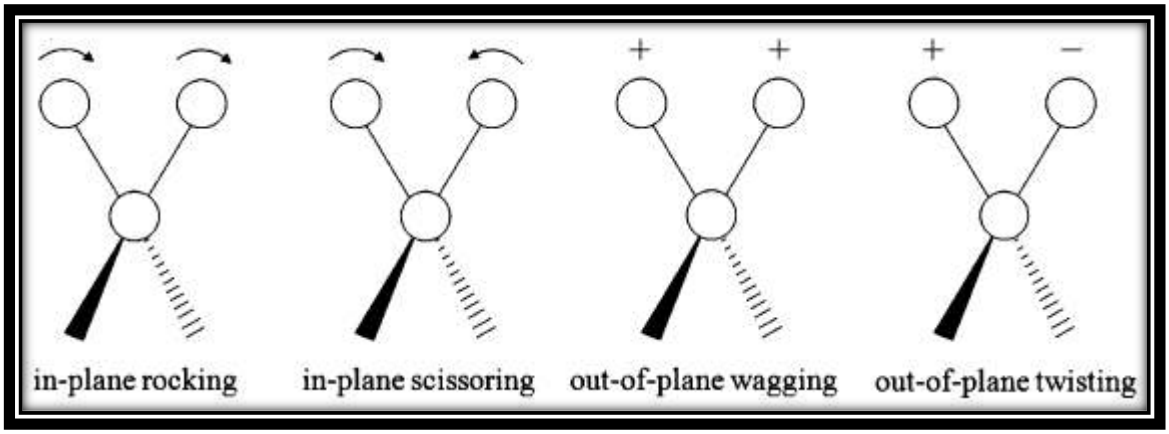

Figure 2.4 Vibrating bends the symbols "+" and "-" represent movement towards the paper and away from the paper, respectively (Ojeda and Dittrich 2012).

2.4.3 Torsion vibration (τ)

A torsional vibration (or torsion) is an internal motion involving four bonded atoms. The bond between two atoms are shown in figure (2.5), BC in this figure, define an axis of rotation that the other two atoms can rotate about. The relative position of those terminal atoms, A and D, define a dihedral angle that specifies the configuration of the atoms. A pure torsional vibration does not change any the molecule's lengths of bonds or bond angles. The value of the dihedral angle has a range $\Phi = [0°, 360°]$

Figure 2.5 Dihedral angle definitions (Coates 2006)

2.5 Molecular Modeling with Quantum Mechanical Methods

2.5.1 Quantum mechanics equation of motion: Schrodinger equation

The basis for studies of the electronic structure of materials is the Schrödinger equation, which is time independent. The wave function (Ψ) may be used to characterize the state of any system. Which in turn depends on the electrons and nuclei positions in the system (S Radhi 2012). This wave function is computed by solving Schrödinger equation numerically or mathematically, and the solution gives the system's overall energy and some physical properties. This equation is represented as follows (Al-Sarraji 2014, Al-kaissy 2011):

$$\hat{H}\Psi = E\Psi \tag{2.8}$$

Where Hˆdenotes the Hamiltonian operator, Ψ denotes the wave functions of all involved particles, and E denotes the particle's overall energy.

The Hamiltonian operator is given by:

$$\hat{H} = \hat{T} + \hat{V} \tag{2.9}$$

The kinetic energy operator in this case is Tˆ, while the potential energy operator is Vˆ.

$$\hat{T} = \frac{1}{2m}\left(\hat{P}_x^2 + \hat{P}_y^2 + \hat{P}_z^2\right) \tag{2.10}$$

Where P is the particle and m is the linear momentum operator mass.

$$\hat{P}_x = -i\hbar\,\frac{\partial}{\partial x}. \qquad \hat{P}_y = -i\hbar\frac{\partial}{\partial y}. \qquad \hat{P}_z = -i\hbar\frac{\partial}{\partial z} \tag{2.11}$$

Equation (2.11) is substituted for equation (2.10), and the outcome is:

$$\hat{T} = \frac{-\hbar^2}{2m}\nabla^2 \tag{2.12}$$

Where, $\nabla^2 = \frac{\partial^2}{\partial x^2} + \frac{\partial^2}{\partial y^2} + \frac{\partial^2}{\partial z^2}$ is the Laplacian operator.

Equations (2.2) and (2.5) are substituted for equation (2.1) to produce (M.S, William 2003):

$$\left[\frac{-\hbar^2}{2m}\nabla^2 + \hat{V}\right]\Psi = E\Psi \qquad (2.13)$$

The solution of the time-independent Schrödinger equation is a key issue in quantum mechanical computations (Khalaf 2013). Only the simplest systems allow for a precise solution to the Schrödinger equation. Since bigger systems are frequently the focus of quantum mechanical computations, the issue must be simplified to approximation solutions to the equation (Meyer 1992).

2.5.2 Born-oppenheimer approach

The idea that it is possible to distinguish between the nuclear motion and the electronic motion in molecules is known as the Born-Oppenheimer approximation. Consequently, the two halves of each molecule's wave function are as follows:

$$\Psi_{total} = \psi_{electron} * \psi_{nucleus} \qquad (2.14)$$

It is commonly known that the nucleus weighs far more than electrons. Three to four orders of mass separate the nucleus from the electron. The nuclear motion might be thought of as stationary since it moves so much more slowly than the electronic motion. The kinetic energy of nuclei is removed, and the potential energy of nuclei-nuclei may be thought of as fixed. This allows the Hamiltonian operator to be simplified as follows by excluding the kinetic energy of nuclei and the potential energy of nuclei from the Hamiltonian operator $\hat{H}$ (C. J. Cramer 2004):

$$\hat{H} = \hat{T} + \hat{V} + \hat{V}_{ee} \qquad (2.15)$$

There are now just three energy operators remaining in the simplified equation. They

are electron-electron interaction energy $\hat{T}$ and electron kinetic energy, respectively. $\hat{V}_{ee}$, and the energy of electron-nuclear interaction V. Actually, the system may be thought of as being composed of all electrons travelling inside a potential field of fixed-position nuclei. As a result, calculating a molecule's total energy is significantly simplified, and calculations of massive molecules' wave functions are now possible (Jensen).

2.5.3 Slater determinate

After John Slate, a spin orbital determinant is known as a Slater determinant. The n electrons are placed among the n spin orbitals in all n! conceivable configurations as a result of increasing the determinant, yielding n! Hartree Products, each with a distinct sign. As needed by the antisymmetry principle, this guarantees that the electrons are indistinguishable. The orbitals that make up the Slater determinant are how they are obtained. The Hartree-Fock theory serves this purpose by demonstrating how to apply the Variational Theorem to select orbitals that minimise total electronic energy. The linear combination of atomic orbitals approach, often known as the LCAO method, expands the spatial orbitals as a linear combination of contracted Gaussian-type functions centred on the individual atoms. This enables the so-called Hartree-Fock Roothan process to convert the integro-differential equations of the Hartree-Fock theory into linear algebra equations (Kaxiras 2003).

How may we increase the wave function's adaptability? Two methods exist: In order to generate even better molecular orbitals, one should (1) utilise a bigger atomic orbital basis set and (2) represent the wave function as a linear combination of several Slater determinants with various orbitals. The latter strategy is applied in the post-Hartree-Fock electron correlation techniques coupled-cluster method, many-body perturbation theory, and configuration interaction (Kaxiras 2003).

According to the Pauli principle, Slater demonstrated that spin-orbitals arranged as a determinant change sign on electron exchange. The Slater determinant can be given as below for the configuration in which each of the Ne electrons fills one different spin-orbital.

$$\Psi(\chi_1, \chi_2, \cdots, \chi_{N_e}) = \frac{1}{\sqrt{N_e}} \begin{vmatrix} \psi_1(\chi_1) & \psi_1(\chi_2) & \cdots & \psi_1(\chi_{N_e}) \\ \psi_2(\chi_1) & \psi_2(\chi_2) & \cdots & \psi_2(\chi_{N_e}) \\ \vdots & \vdots & \ddots & \vdots \\ \psi_{N_e}(\chi_1) & \psi_{N_e}(\chi_2) & \cdots & \psi_{N_e}(\chi_{N_e}) \end{vmatrix}$$

Often the normalization constant $(N_e!)^{-1/2}$ is omitted and only the diagonal elements are written.

$$\Psi(\chi_1, \chi_2, \cdots, \chi_{N_e}) = |\psi_1(\chi_1)\psi_2(\chi_2) \cdots \psi_{N_e}(\chi_{N_e})|$$

Now, one further approximation made, by assuming that there is just one Slater determinant in the trial wave function. This suggests that electron correlation is ignored, or to put it another way, that the electron-electron repulsion is only taken into account as an average effect, as will be demonstrated later. The Hartree-Fock equations may be derived using the variational principle after choosing a single-determinant trial wave function by minimising the energy (Jensen).

2.6 Molecular Modeling Methods

2.6.1 Molecular mechanical method

With the use of potential functions derived from classical physics, the potential energy surface for a certain arrangement of atoms is computed using the computational technique known as molecular mechanics. They are referred to as a force-field. Molecular mechanics is predicated on the following hypotheses: It regards the nucleus itself and the electrons around it as perfect spheres. Molecules' bonds are thought of having spring-like structures. The potential energy function is the result of adding the separate functions for bond stretching, angle bending, torsional energies, and non-bonding interactions. Potential functions are dependent on experimental data like force constants and

equilibrium values (van der Kamp and Mulholland 2013). The molecular mechanics-generated potential functions have no definitive significance and are just useful for comparing various molecule combinations (Lonsdale *et al.* 2012).

2.6.2 Semi empirical method

J. A. Pople created the earliest semi empirical molecular orbital, or MO, approaches, such as CNDO, INDO, and NDDO (Pople and Segal 1966) and his team at a period when computers could only handle the smallest systems' worth of Ab initio computations. These techniques were designed to mimic other electrical characteristics, such the dipole moment, rather than molecule geometries and temperatures of formation. The simplest approach is CNDO (Complete Neglect of Differential Overlap), evaluates the electron repulsion integrals on the supposition that the atomic orbitals are spherically symmetric. The only way to account for the directionality of p-orbitals is through the one electron resonance integrals; the size is determined by the orbitals' orientations and distances as well as by a constant that is specific to each type of bond. The INDO stage comes next (Intermediate Neglect of Differential Overlap) included one center repulsion integrals between atomic orbitals on the same atom as a rough approximation. The directionality of the atomic orbitals was first accounted for in the calculation of the repulsion integrals using the NDDO (Neglect of Diatomic Differential Overlap) approximation. In this instance, the overlap between atomic orbitals on the same atom was taken into account in the three- and four-center integrals. Pople and Beveridge provide descriptions that are more detailed. J. A. Pople and (Beveridge 1970) and by Dewar (Dewar 1969 , Murrell and Harget 1972) The MO techniques created by M. J. S. Dewar and his team expressly for use in organic research include the semi empirical approaches MINDO/3, MNDO, and AM1 (Dewar 1969 , Murrell and Harget 1972).

2.6.3 Ab initio method

It's a Latin word meaning (from the beginning). The foundation of this group is this. It is based on the Schrodinger equation, whose zero-point solutions are fully dependent on the ideas of quantum mechanics. When the Schrodinger equation is solved, we obtain energy and a wave function, which explain how the electron moves within the molecule. The electronic distribution of electrons in the molecule is expressed mathematically by the resulting wave function. This distribution may be used to determine the polarity of the molecule calculated. It can also calculate molecular spatial structure, vibrational energy, ionization energy, electronic affinity, dipole moment and other characteristics (Crawford 2007).

Schrodinger's equation is the nucleus or building block of quantum physics and thus of chemistry theory and arithmetic authored in 1925 and published in 1926 by Erwin Schrodinger. When the electron was initially described as being in a wave state (Hehre 2003):

$$\hat{H}\psi(\vec{r},t) = E\psi(\vec{r},t) \tag{2.16}$$

Where $\hat{H}$ the chemical system's overall wave function, the Hamiltonian operator, Ψ and the energy.

The developed expression of the Hamiltonian operator is:

$$\hat{H} = -\frac{1}{2}\sum_{i=1}^{N}\nabla_i^2 - \sum_{A=1}^{M}\frac{1}{2m_A}\nabla_A^2 - \sum_{i=1}^{N}\sum_{A=1}^{M}\frac{Z_A}{r_{iA}} + \sum_{i=1}^{N}\sum_{j>i}^{N}\frac{1}{r_{ij}} + \sum_{A=1}^{M}\sum_{B>A}^{M}\frac{Z_A Z_B}{r_{AB}} \tag{2.17}$$

$$\hat{H}_{total} = \hat{T}_{elec.} + \hat{T}_{nucl.} + \hat{V}_{nucl.\ elec.} + \hat{V}_{elec.\ elec.} + \hat{V}_{nucl.\ nucl.} \tag{2.18}$$

The Coulomb attraction between nuclei and electrons is denoted by $\widehat{V}_{ne}$, the Coulomb repulsion between electrons is denoted by, ($\widehat{V}_{ee}$) and the Coulomb attraction between nuclei is denoted by$\widehat{V}_{nn}$. The following are examples of the kinetic energy operators:

$$\widehat{T}_e = -\frac{\hbar^2}{2m_e}\sum_i \nabla_i^2 \ldots\ldots \quad (2.19)$$

$$\widehat{T}_n = -\frac{\hbar^2}{2\,M_A}\sum_A \nabla_A^2 \ldots\ldots \quad (2.20)$$

When M_E represents the nuclear mass and M_A represents the electron mass, ∇_i^2 is the i-electrons Laplacian operator, which has the following form in Cartesian coordinates:

$$\nabla_i^2 = \frac{\partial^2}{\partial x_i^2} + \frac{\partial^2}{\partial y_i^2} + \frac{\partial^2}{\partial z_i^2} \quad \ldots\ldots\ldots \quad (2.21)$$

The following are the possible energy operators:

$$\widehat{V}_{nn} = \sum_{A<B} Z_A Z_B \frac{e^2}{R_{AB}} \quad (2.22)$$

$$\widehat{V}_{ne} = -\sum_A \sum_i Z_A \frac{e^2}{r_{Ai}} \quad (2.23)$$

$$\widehat{V}_{ee} = \sum_{i<j} \frac{e^2}{r_{ij}} \quad (2.24)$$

Where $r_{ij} = \left|\vec{r_\imath} - \vec{r_j}\right|$ and Z_A is the charge of the nucleus A, r_{Ai} is the separation between the nucleus and the electron, r_{ij} is the separation between i and j electrons, and R_AB is the separation between a and b nuclei. Schrodinger equation is known as an equation is not solvable except for single-electron systems such as hydrogen. Therefore, to answer this problem, various approximations in mathematics are required. The simplest of these approximations is the Hartree-Fock approximation, which relies on the central field principle. This shows that the Coulombic electron-electron resistance is taken into account when integrating the attraction component. Instead of the explicit repulsion

interaction, this gives the average impact of the repulsion (Kaupp 2001). The approximate energies obtained in this variation calculation are all equal to or higher than the actual energy. Hartrees are used to measure the energy (1 Hartree = 27.2116 eV). The fact that this approach divides the complex one-electron Schrödinger equation into several smaller one-electron equations is one of its benefits. A single-electron wave function between an orbital and an energy, known as an orbital energy, is produced by solving each one-electron equation. An electron's behaviour in the net field created by all the other electrons is described by its orbital. Due to the requirement that the wave function be defined by some mathematical function, which is precisely known for only a small number of one-electron systems, the second approximation in HF calculations is necessary. By using the so-called Hartree-Fock equations, this technique reduces the n-particle issue to a collection of one particle eigenvalue problems:

$$\hat{f}_i \Psi_i = \varepsilon_i \Psi_i \tag{2.25}$$

Where Ψ_i is an Eigen function of the operator $\hat{f}_i$, which is also known as the Fock operator and ε_i is the associated energy. According to this definition, each electron's Fock operator is:

$$\hat{f}_i = -\frac{1}{2} - \sum_A^M \frac{Z_A}{r_{iA}} + V_{HF}(i) \tag{2.26}$$

Where $V_{HF}(i)$ is known as the Hartree-Fock potential, This explains the typical repellent potential each electron experiences as a result of the other n-1 electrons and has two components, namely the coupling factor $\hat{J}_1(j)$ as well as the exchange operator $\hat{K}_1(j)$:

$$V_{HF}(i) = \sum_j^N \left(\hat{J}_1(j) - \hat{K}_1(j)\right) \tag{2.27}$$

The method's primary drawback is its disregard for electron-electron communication effect so it has been developed a variety of theories and techniques that start from the method of Hartree –Fock and then add the correlation of these methods The SCF approach is short for self-consistent field. When adding electronic bonding (the effect of electrons among them), this increases the accuracy calculations whether it is in the energy calculation or the calculation of the spatial shape, in addition, this type of method is considered much slower than the molecular mechanics methods but is relatively considered more accurate (Rogers 2003).

2.6.4 Hartee-Fock method self-consistent field (SCF) theory

Hartree-Fock is one of the most important approximations used to resolve the equation developed by Schrödinger for each and every system's electron. It serves as the foundation for molecular orbital (MO) theory, which states that each electron's motion may be explained by a single-particle function (orbital) that is independent of the other electrons' immediate movements (Yong 2001).

Hartree assumed that overall wave function could be generally approximated as a series of one electron wave function (Rogers 2003). The equations known as the Hartree-Fock equations:

$$\hat{f}_i \Psi_i = \varepsilon_i \Psi_i \qquad (2.28)$$

Where Ψ_i is an eigenfunction of the operator $\hat{f}_i$, which is also known as the Fock operator and ε_i is the corresponding energy.

The computed approximate energies are all more than or equal to the measured precise energy. Hartrees are used to measure the energy (1 Hartree = 27.2116eV) (Fock 1930).

The Hartree-Fock approximation approach posits that wave function of a system of (n electrons) may be expressed by Slater determinant. This determinant is a statement that the spin of every electron complies with Pauli Exclusion Theory. The wave function of Hartree-Fock is commonly modeled as a Slater determinant.

$$\Psi\ (1.2.\ldots.\mathrm{n}) = \frac{1}{\sqrt{\mathrm{n!}}}\begin{vmatrix} \Psi_1(\chi_1) & \Psi_2(\chi_1) & \cdots & \Psi_\mathrm{n}(\chi_1) \\ \Psi_1(\chi_2) & \Psi_2(\chi_2) & \cdots & \Psi_\mathrm{n}(\chi_2) \\ \vdots & \vdots & \ddots & \vdots \\ \Psi_1(\chi_\mathrm{n}) & \Psi_1(\chi_\mathrm{n}) & \cdots & \Psi_\mathrm{n}(\chi_\mathrm{n}) \end{vmatrix} \qquad (2.29)$$

Where Ψ, which produces electrical waves, and $\frac{1}{\sqrt{\mathrm{n!}}}$ is a normalization factor (Yong 2001).

2.6.5 Density functional method

One of the most well-liked and effective quantum mechanical methods for computing the electrical composition of matter is density-functional theory (Valone 2010).

In 1927, the functional predecessor to The Thomas-Fermi model, devised by Thomas and Fermi, provided the basis for density theory. Thomas and Fermi computed an atom's energy by modelling its motion energy as a function of electron density. DFT predicts a wide range of molecular features, including molecular structures, vibrational frequencies, ionisation energies, electric and atomization energies, reaction routes, and magnetic properties, among others (Rogers 2003, Fitts 1999).

DFT approaches are gaining popularity since the results achieved are equivalent to those obtained using Ab initio methods because of the drastically reduced CPU time. The DFT method differs from other methods which are based on HF studies in the sense that the electron density, rather than a wave function, is employed to determine energy (Sholl and Steckel 2011, Bransden and Joachain 2003).

DFT calculates the characteristics of a large number of particles in relation to their electron density $\rho(r)$. The density of electrons of a given state the number of electrons per unit volume is defined. It is reliant on only regardless of the number of electrons in the system, as follows (Mueller 2007):

$$N = \int \rho(\vec{r})\, d\vec{r} \qquad (2.30)$$

The electron density is defined as well as the chance of discovering an electron(s) in a particular region, and when the electron's distance from the nucleus is approaches infinity, it approaches zero. As the number of electrons rises, theoretically speaking, the wave function approaches get substantially more difficult (Kohanoff and Gidopoulos 2003).

DFT's core notions are based on ground state energy, and all other ground level electronic parameters are defined specifically by electron density. Furthermore, the system's precise ground state correlates to the electrical densities for least total energy (Mueller 2007)

2.7 Potential Energy Surface

It is conceivable to have sites where two potential power surfaces U(R) have the same energy when computing multiple potential energy surfaces for a system. What occurs afterwards is very interesting to chemists and will be covered in this section. Hund proposed the rule against crossing (Hund 1927) was developed by Neumann and Wigner in 1929 (Neumann and Wigner 1929). It says that potential energy curves that correspond to electrical states of the same symmetries cannot intersect in a diatomic molecule with an endlessly slow change in internuclear distance. The new energies resist each other when two wave functions are merged to generate a better wave function the two wave functions are combined and break apart when two potential energy surfaces draw near together along the reaction coordinate. An averted crossing point is the point of closest approach. The avoided crossing points develop as a result of the adiabatic electronic states

around the avoided crossing point being mixes of molecular orbitals from two states. The mixing of the two molecular orbitals causes two states to reject each other, resulting in state separation. A diabatic surface is one on which the real junctions are replaced for the averted crossing. If the nuclei travel slowly, they will most likely follow a single adiabatic surface. However, if the nuclei have enough velocity, the Born-Oppenheimer approximation breaks down, and the nuclei can essentially disregard the gap in the avoided crossing and just cross over to the opposite isothermal surface, adopting that configuration. This is referred to as non-adiabatic behaviour. However, if the symmetries of two potential energy surfaces are sufficiently different, they can cross. Hund proposed that if two potential energy surfaces intersect, the electronic state at the crossing point must be degenerate (Hund 1927).

2.8 Geometry optimization

Geometry optimizations determine the molecular structure coordinates that indicate the potential energy minimum. The optimized coordinates meet the equation for a potential energy U and Cartesian coordinates r_j:

$$\partial U/\partial r_j = 0 \quad \ldots\ldots\ldots \quad (2.31)$$

The following are the goals of a geometry optimization calculation: to characterize a potential energy minimum (a geometry optimization produces an entirely novel structure at a minimum; studying the atomic regulates and energy of that structure can be done); to obtain a new stable structure as a starting point for just one location, semi-empirical estimation (this provides a large set of structural and electronic properties; and to prepare a molecule for a molecular diffraction calculation (Kwon 2012).

2.9 Slater type orbitals

Have a variety of appealing characteristics, the most of which are linked with how closely they mimic hydrogenic atomic orbitals. When the fundamental set functions are STOs, there is no analytical solution for the generic four-index integral. A typical (STO) is written as (Rogers 2003):

$$\chi^{STO} = Nr^{n-1}e^{-\xi r}Y_{lm}(\theta, \varphi) \quad \ldots\ldots\ldots \quad .(2.32)$$

In this case, n is a primary quantum number and N is the normalization constant. ξ is a constant linked to the nucleus's effective charge, i.e. the nuclear charge being partially protected by electrons. Y_{lm} is A spherical harmonic that describes the wave function's angular component. Slater type functions provide proper behaviour near the nucleus with a discontinuous behaviour at r 0. A Slater type orbital, or STO, is the perfect solution to the Schrödinger equation for the hydrogen atom the form exp (-ξr) (Valone 2010).

2.10 Gaussian type orbitals

GTOs can be written in terms of Cartesian coordinates as (Fitts 2002):

$$X^{GTO} = Nx^{l_x}y^{l_y}z^{l_z}e^{-\xi r^2} \ldots\ldots\ldots \quad (2.33)$$

The sum of l_x, l_y and l_Z determines the type of orbitals, ξrepresents The orbital number that indicates how compact. The r^2dependence in the exponent is a weakness of the (GTO) in comparison to the Slater-Type Orbitals (STO). GTOs have two major issues. The first issue is that GTO behaves incorrectly near the nuclei at r 0. The second issue is that GTO falls off too quickly further from the nuclei when compared to STO. As a result, the tail of the wave function in the GTO is poorly represented.

A rough estimate suggests that three times as many GTOs as STOs are needed to achieve the same degree of precision. One downside of STOs is the difficulty in computing many-

center integrals such as Coulomb and HF-exchange terms. As a result, it has no place in contemporary wave function-based quantum chemical codes. The fact that the sum of two Gaussian functions is another Gaussian function is one of the advantages of the Gaussian basis set. As a consequence, the analytical solution for the Gaussian functions is accessible for the computation of Coulomb and HF-exchange terms. As a result, the GTO basis function is widely used in HF and related approaches because relatively efficient algorithms exist for analytically computing many-center integrals.

To enhance GTO basis sets, a contracted GTO basis set is typically used, in which numerous basic Gaussian functions are merged to provide a contracted Gaussian function (CGF) (Clementi *et al.* 2012):

$$\chi_j^{CGF} = \sum_i^M C_{ij}\chi_a^{GTO} \quad \ldots\ldots\ldots \quad (2.35)$$

M is the number of Gaussian primitives utilised in a linear combination in this case, and C_{ij} are the orbital expansion coefficients. Gaussian's basis sets are divided into three types: minimum basis sets, split polarity sets, and full valence sets polarization and diffuse functions and others (Valone 2010, Clementi *et al.* 2012).

2.11 Basis Sets

A basis set is a collection of functions used to characterise the geometry of an atom's orbitals. Linear combinations of basis functions provide Molecular orbitals and complete wave functions. A preset basis set is used by the majority of semi empirical approaches. A basis set must be given when performing ab initio or density functional theory computations.

Although a basis set may be created from scratch, most computations are performed using existing basis sets. The type of computation used and the basis set used are the two most important aspects in influencing the correctness of the findings. The basic set functions

must be chosen in order to have a chemically usable form. Although a basis set may be created from scratch, most computations are performed using existing basis sets. The type of computation used and the basis set used are the two most important aspects in influencing the correctness of the findings. The basic set functions must be chosen in order to have a chemically usable form. That is, the functions should have large amplitudes in parts of space where the electron probability density (the wave function) is high, ion and small amplitudes in regs where the probability density is low (Marenich *et al.* 2014) That is, the functions should have large amplitudes in parts of space where the electron probability density (the wave function) is high, ion and small amplitudes in regSeveral approaches exist for determining electron distribution around the nucleus, including the use of hydrogen similarity functions, which are based on the Schrodinger equation for the hydrogen atom, or polynomial functions with customizable coefficients. In addition, we have Slater and Gauss functions (sometimes known as Gaussian functions).

3. MATERIALS AND METHODS

The approximate geometry of (E)-4-((p-tolilimino)methyl)phenyl acrylate Schiff The Gaussian View 5.0 molecule imaging program will be used to create a three-dimensional base, and the spatial arrangement of the atoms in the molecule will be determined. All theoretical calculations will be made Gaussian 09 and Gauss View 5.0 is included in the package program. After the geometry of the molecule has been drawn

a) Geometric optimization will be done to find its stable structure.
b) Vibration frequencies will be calculated
c) Vibration frequencies will be marked using the Gauss View 5.0 program.
d) Chemical shifts will be calculated by NMR spectroscopy.
e) HOMO-LUMO molecular orbital energies will be calculated.
f) Nonlinear optical properties (NLO) will be calculated.

After marking the frequencies of vibration of the compounds and calculating their The chemical shifts of NMR molecules, as well as their nonlinear optical characteristics (NLO) and HOMO-LUMO molecular orbital energies, will be computed. All calculations will be performed using the DFT/B3LYP technique with the basis set 6-311++G (d,p).

4. RESULTS AND DISCUSSION

4.1 Geometrical Optimization Of The (E)-4-((p-tolylimino) methyl) phenyl acrylate compound

The three-dimensional geometry of the molecule was drawn with the program Gauss View 5.0. Then, full geometry optimization was performed with the DFT/B3LYP/6-311+G (d, p) method and the lowest energy structure of the molecular system was found (Figure 4.1).

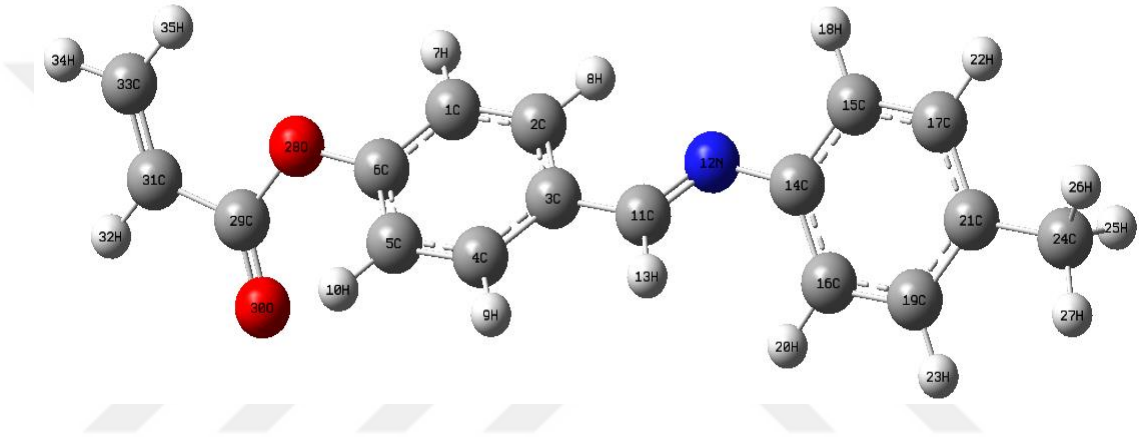

Figure 4.1 Optimized structure of the (E)-4-((p-tolylimino) methyl) phenyl acrylate compound

Bond lengths, bond angles, and torsion angles are all calculated of the compound are given in Table 4.1. According to our knowledge of the literature so far, no experimental data on the structural parameters of the compound have been found. For this reason, the comparison of certain structural parameters was made according to similar molecules studied in the literature.

The N-C bond length was experimentally determined as 1.470Å they found 1.468Å theoretically by (Alyar *et al.* 2012). In this study, the N-C bond length was calculated as 1.405Å.

Alyar measured the C-C bond length as 1.392Å experimentally and calculated 1.402Å theoretically. In this study, the bond C-C length was calculated as 1.394Å.

Table 4.1 Molecular geometric parameters (bond lengths, bond and torsion angles) of (E)-4-((p-tolylimino) methyl) phenyl acrylate compound

Bond Length	B3LYP-6311++G(d, p)	Bond Angles	B3LYP-6311++G(d,p)	Torsion Angle	B3LYP-6311++G(d,p)
C1-C2	1.386	C2-C1-C6	119.6	C6-C1-C2-C3	-0.028
C1-C6	1.394	C2-C1-H7	121.2	C6-C1-C2-H8	179.939
C1-H7	1.083	C6-C1-H7	119.1	H7-C1-C2-C3	179.906
C2-C3	1.403	C1-C2-C3	120.4	H7-C1-C2-H8	-0.125
C2-H8	1.082	C1-C2-H8	120.7	C2-C1-C6-C5	0.232
C3-C4	1.401	C3-C2-H8	118.8	C2-C1-C6-O28	176.241
C3-C11	1.467	C2-C3-C4	118.7	H7-C1-C6-C5	-179.703
C4-C5	1.391	C2-C3-C11	121.7	H7-C1-C6-O28	-3.695
C4-H9	1.085	C4-C3-C11	119.4	C1-C2-C3-C4	-0.045
C5-C6	1.390	C3-C4-C5	121.3	C1-C2-C3-C11	-179.942
C5-H10	1.080	C3-C4-H9	119.5	H8-C2-C3-C4	179.985
C6-O28	1.393	C5-C4-H9	119.1	H8-C2-C3-C11	0.088
C11-N12	1.276	C4-C5-C6	118.6	C2-C3-C4-C5	-0.081
C11-H13	1.098	C4-C5-H10	120.7	C2-C3-C4-H9	-179.989
N12-C14	1.405	C6-C5-H10	120.5	C11-C3-C4-C5	179.818
C14-C15	1.402	C1-C6-C5	121.1	C11-C3-C4-H9	-0.089
C14-C16	1.402	C1-C6-O28	116.3	C2-C3-C11-N12	2.113
C15-C17	1.388	C5-C6-O28	122.3	C2-C3-C11-H13	-178.841
C15-H18	1.083	C3-C11-N12	122.8	C4-C3-C11-N12	-177.784
C16-C19	1.392	C3-C11-H13	115.5	C4-C3-C11-H13	1.262
C16-H20	1.084	N12-C11-H13	121.6	C3-C4-C5-C6	0.277
C17-C21	1.401	C11-N12-C14	120.4	C3-C4-C5-H10	179.661
C17-H22	1.085	N12-C14-C15	118.02	H9-C4-C5-C6	-179.814
C19-C21	1.397	N12-C14-C16	123.5	H9-C4-C5-H10	-0.431

Table 4.1 (Continued)

C19-H23	1.085	C15-C14-C16	118.4	C4-C5-C6-C1	-0.354
C21-C24	1.509	C14-C15-C17	120.5	C4-C5-C6-O28	-176.118
C24-H25	1.095	C14-C15-H18	118.5	H10-C5-C6-C1	-179.739
C24-H26	1.093	C17-C15-H18	120.8	H10-C5-C6-O28	4.497
C24-H27	1.092	C14-C16-C19	120.4	C1-C6-O28-C29	132.014
O28-C29	1.371	C14-C16-H20	119.8	C5-C6-O28-C29	-52.030
C29-O30	1.204	C19-C16-H20	119.7	C3-C11-N12-C14	-177.138
C29-C31	1.480	C15-C17-C21	121.3	H13-C11-N12-C14	3.873
C31-H32	1.083	C15-C17-H22	119.2	C11-N12-C14-C15	-143.392
C31-C33	1.332	C21-C17-H22	119.4	C11-N12-C14-C16	39.216
C33-H34	1.083	C16-C19-C21	121.4	N12-C14-C15-C17	-179.916
C33-H35	1.083	C16-C19-H23	119.1	N12-C14-C15-H18	1.003
		C21-C19-H23	119.4	C16-C14-C15-C17	-2.389
		C17-C21-C19	117.7	C16-C14-C15-H18	178.530
		C17-C21-C24	120.9	N12-C14-C16-C19	178.834
		C19-C21-C24	121.3	N12-C14-C16-H20	0.838
		C21-C24-H25	111.1	C15-C14-C16-C19	1.452
		C21-C24-H26	111.35	C15-C14-C16-H20	-176.544
		C21-C24-H27	111.38	C14-C15-C17-C21	1.836
		H25-C24-H26	107.2	C14-C15-C17-H22	-178.813
		H25-C24-H27	107.4	H18-C15-C17-C21	-179.105
		H26-C24-H27	108.001	H18-C15-C17-H22	0.245
		C6-O28-C29	121.01	C14-C16-C19-C21	0.067
		O28-C29-O30	124.03	C14-C16-C19-H23	-179.379
		O28-C29-C31	112.02	H20-C16-C19-C21	178.065
		030-C29-C31	123.9	H20-C16-C19-H23	-1.381
		C29-C31-H32	113.1	C15-C17-C21-C19	-0.282
		C29-C31-C33	125.04	C15-C17-C21-C24	177.888
		H32-C31-C33	121.7	H22-C17-C21-C19	-179.632

The C-O bond length was found 1.364Å theoretically by (S. Alyar and Sevki 2014). In this study, the C-O bond length was calculated as 1.393Å.

These results show us that our theoretical calculations are compatible with the experimental and theoretic data found in the literature for similar molecular systems.

4.2 Vibrational Assignment of (E)-4-((p-tolylimino) methyl) phenyl Acrylate

In this section of our thesis, we formed and interpreted the responsibilities of the fundamental frequency of vibration computed for the stable structure of the molecular structure (E)-4-((p-tolylimino) methyl) phenyl acrylate at minimal energy. The 35 atom molecule (E)-4-((p-tolylimino)methyl) phenyl acrylate compound exhibits 99 fundamental vibration frequencies. The experimental FT-IR spectrum of the (E)-4-((p-tolylimino) methyl) phenyl acrylate chemical compound molecule's is displayed in Figure 4.2 (Sılku 2014). Theoretical and experimental vibration frequencies are given in on the Table 4.2.

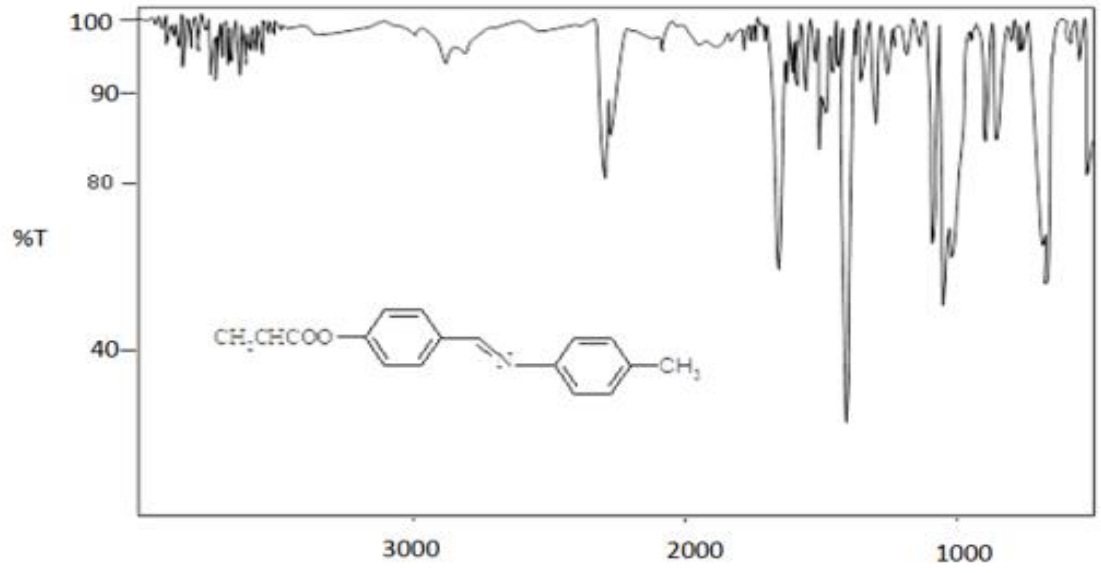

Figure 4.2 FT-IR spectrum of (E)-4-((p-tolylimino) methyl) phenyl acrylate compound

Table 4.2 Theoretical and experimental (FT-IR) vibration frequencies of the (E)-4-((p-tolylimino) methyl) phenyl acrylate

Mode	Exp. (Sılku 2014)	Calculated	Intensity	Descriptions
99		3240	4.60	υ_{as} ($C_{33}H_2$) + υ ($C_{31}H_{32}$)
98		3218	3.73	υ $(CH)_{R1}$
97		3204	3.18	υ $(CH)_{R1}$
96		3188.35	3.03	υ $(CH)_{R1}$
95		3187.89	3.40	υ ($C_{31}H_{32}$) + υ ($C_{33}H_{35}$)
94		3187	6.53	υ $(CH)_{R2}$
93		3179	9.46	υ $(CH)_{R2}$
92		3167	8.28	υ $(CH)_{R1}$
91		3156	23.28	υ $(CH)_{R2}$
90		3155	1636	υ $(CH)_{R2}$
89		3148	4.81	υ_s ($C_{33}H_2$) + υ ($C_{31}H_{32}$)
88		3099	16.73	υ_{as} ($C_{24}H_2$) + υ_s ($C_{24}H_2$)
87	3033	3071	20.08	υ_s ($C_{24}H_2$) + υ_{as} ($C_{24}H_2$)
86		3019	47.03	υ_s ($C_{24}H_2$)
85	2919	3005	43.36	υ ($C_{11}H_{13}$)
84	1749	1791	264.56	υ ($C_{29}=O_{30}$) + υ ($C_{31}=C_{33}$) + β ($C_{33}H_2$) + β ($C_{29}CH_{32}$)
83		1687	96.16	υ ($C_{11}=N_{12}$) + υ $(CC)_{R1,2}$ + β (C_3CH_{13})
82	1652	1680	10.22	υ ($C_{31}=C_{33}$) + υ ($C_{29}=O_{30}$) + β ($C_{33}H_2$) + β ($C_{29}CH_{32}$)
81		1647	16.42	υ $(CC)_{R1,2}$ + υ ($C_{11}=N_{12}$) + β $(CCH)_{R1,2}$
80		1636	57.67	υ $(CC)_{R1,2}$ + υ ($C_{11}=N_{12}$) + β $(CCH)_{R1,2}$ + β ($C_{11}NH$)
79		1614	47.09	υ $(CC)_{R1}$ + υ ($C_{11}=N_{12}$) + β (C_5CH_9) + β (C_2CH_7) + β (C_4CH_{10})
78		1601	2.81	υ $(CC)_{R2}$ + β ($C19CH_{20}$) + β ($C_{19}CH_{20}$) + β ($C_{17}CH_{18}$) + β ($C_{21}CH_{26}$) + β ($C_{21}CH_{27}$) + β ($C_{24}H_2$)
77		1539	137.45	υ $(CC)_{R1,2}$ + β $(CCH)_{R1,2}$ + υ (C_3C_{11}) + υ ($C_{14}N_{12}$) + υ (C_6O_{28}) + υ ($C_{21}C_{24}$)
76		1531	0.95	υ $(CC)_{R1,2}$ + β $(CCH)_{R1,2}$ + υ (C_3C_{11}) + υ ($C_{14}N_{12}$) + υ (C_6O_{28}) + υ ($C_{21}C_{24}$)
75		1494	8.22	υ $(CC)_{R2}$ + β ($C_{24}H_2$)
74		1488	6.95	β ($C_{24}H_2$) + γ ($C_{24}H_{25}H_{26}$)
73		1447	6.68	υ $(CC)_{R1,2}$ + υ (C_{11}=N_{12}) + β $(CCH)_{R1,2}$ + β ($C_{33}H_2$)
72		1439	28.79	υ $(CC)_{R2}$ + υ ($C_{31}=C_{33}$) + β ($C_{33}H_2$) + β ($C_{24}H_2$)
71		1438	29.12	υ $(CC)_{R1,2}$ + β $(CCH)_{R2}$ + β ($C_{33}H_2$) + β ($C_{24}H_2$)
70		1414	0.09	γ ($C_{24}H_2$)
69		1402	11.54	υ $(CC)_{R1,2}$ + υ (C_{11}=N_{12}) + β ($CN_{12}H$)
68		1337	0.25	υ $(CC)_{R1,2}$ + β $(CCH)_{R2}$ + β ($CN_{12}H$) + β (C_6CO_{28})
67		1333	3.71	υ $(CC)_{R1,2}$ + β $(CCH)_{R2}$ + β ($C_{21}CH_{27}$) + γ ($C_{24}H_{25}H_{26}$)
66		1325	7.18	υ $(CC)_{R2}$ + β $(CCH)_{R1}$ + γ ($C_{24}H_{25}H_{26}$)
65		1313	10.62	υ ($C_{31}=C_{33}$) +β ($C_{31}CH_{35}$) + β ($C_{33}CH_{32}$)
64		1311	3.63	υ $(CC)_{R1,2}$ + β ($C_{21}CH_{27}$) + γ ($C_{24}H_{25}H_{26}$) + β ($C_{14}CH_{18}$)
63		1268	5.48	υ $(CC)_{R1,2}$ + υ (C_3C_{11}) + υ ($C_{14}N_{12}$) + β (C_2CH_7) + β (C_3CH_{13}) + β (C_3NH_{13})

Table 4.2 (Continued)

62		1251	335.53	$\upsilon (CC)_{R1} + \upsilon (C_6O_{28}) + \upsilon (C_{29}O_{28}) + \upsilon (C_{29}C_{31}) + \beta (C_{29}CH_{32}) + \beta (C_{31}CH_{35}) + \beta (C_{33}H_2) + \beta (C_6CO_{28})$
61		1230	26.67	$\upsilon (CC)_{R2} + \upsilon (C_{21}C_{24}) + \gamma (C_{24}H_2)$
60		1220	651.34	$\upsilon (CC)_{R1,2} + \upsilon (C_6O_{28}) + \upsilon (C_{29}O_{28}) + \upsilon (C_{14}N_{12}) + \beta (CCH)_{R1} + \beta (C_{29}CH_{32}) + \beta (C_{33}H_2)$
59	1202	1214	24.11	$\upsilon (CC)_{R1,2} + \upsilon (C_6O_{28}) + \upsilon (C_{21}C_{24}) + \upsilon (C_{14}N_{12}) + \upsilon (C_3C_{11}) + \beta (C_5CH_9) + \beta (C_2CH_7)$
58		1191	1.31	$\upsilon (CC)_{R2} + \upsilon (C_{14}N_{12}) + \beta (CCH)_{R2}$
57		1181	217.77	$\upsilon (CC)_{R1} + \upsilon (C_6O_{28}) + \beta (CCH)_{R1}$
56		1136	8.29	$\upsilon (CC)_{R2} + \beta (C_{19}CH_{20}) + \gamma (C_{24}H_{25}H_{26})$
55		1126	12.74	$\upsilon (CC)_{R1} + \beta (C_4CH_{10})$
54		1059	12.11	$\beta (C_{21}CH_{25}) + \beta (C_{21}CH_{26}) + \gamma (C_{24}H_{26}H_{27})$
53		1033	211.97	$\upsilon (CC)_{R1} + \upsilon (C_{29}O_{28}) + \beta (C_{33}H_2) + \beta (C_{33}CH)$
52		1031	11.89	$\upsilon (CC)_{R2} + \beta (CCH)_{R2} + \gamma (C_{24}H_2)$
51		1029	42.85	$\upsilon (CC)_{R1} + \beta (CCH)_{R1} + \beta (C_{33}H_2) + \beta (CCC)_{R1} + + \beta (CCH)_{R1}$
50		1027	18.43	$\tau (C_{33}H{=}CH_2)$
49		1009	3.29	$\beta (C_{21}CH_{27}) + \gamma (C_{21}H_2)$
48		1007	36.48	$\gamma (C_{33}H_2)$
47		1001	5.53	$\beta (C_{21}CH_{27}) + \gamma (C_{21}H_2) + \gamma (CH{=}N_{12}) + \tau (CCCH)_R$
46		990	0.72	τ (CCCC)R + τ (CCCH)R
45		977	0.42	τ (CCCC)R + τ (CCCH)R
44		962	1.35	τ (CCCC)R + τ (CCCH)R
43		954	2.12	τ (CCCC)R + τ (CCCH)R
42		912	32.24	β (C33H2) + υs (C31CO28) + τ (CCCC)R + τ (CCCH)R
41		899	34.49	υ (CC)R1,2 + β (C3CH13) + β (C11NH)
40		867	25.13	β (C33H2) + τ (CCCC)R + τ (CCCH)R
39		852	16.71	υ (CC)R1,2 + τ (CCCC)R + τ (CCCH)R
38		842	7.79	τ (CCCC)R + τ (CCCH)R
37		835	4.97	τ (CCCC)R + τ (CCCH)R
36		828	1.44	τ (CCCC)R + τ (CCCH)R
35		823	45.46	γ (C33H2) + τ (CCCH)R
34		806	2.07	β (C29O2) + γ (C33H2) + τ (CCCH)R
33		771	1.83	υ (C21C24) + β (C33H2) + β (CCC)R2
32		735	3.94	τ (CCCC)R + τ (CCCH)R
31		721	3.74	γ (C24H2) + τ (CCCC)R + τ (CCCH)R
30		665	15.01	β (C33H2) + β (CCC)R1
29		657	0.12	β (CC)R2 + β (C33H2)
28		646	0.27	β (CC)R1 + β (C33H2)
27		568	14	β (C31CO) + τ (CCCC)R + τ (CCCH)R
26		548	21.80	τ (CCCC)R + τ (CCCH)R + τ (CCCN) + τ (CNCC)
25		535	2.15	υ (CC)R2 + β (C33H2) + β (C33CC)
24		533	5.07	τ (CCCC)R + τ (CCCH)R + τ (CCCN) + τ (CNCC)
23		504	2.38	γ (C33H2) + τ (C33H=CH2) + τ (C31H=CO)
22		486	5.58	β (C11=CN) + τ (CCCC)R + τ (CCCH)R

ν, bond stretching; β, in-plane angle bending; γ, out -of-plane angle bending; τ is torsion; as is antisymmetric and s is symmetric

When the IR spectrum of the compound numbered (Figure 4.2) is investigated, the peak corresponding to the carbonyl group (>C=O) is seen at 1749 cm^{-1}, were calculated at 1791 cm^{-1} theoretically. The aliphatic C-H stretch at 2919 cm^{-1} and 2850 cm^{-1}, theoretically were calculated at 3005 cm^{-1}. The aromatic and aliphatic –C=C- stretch peaks at 1652 cm^{-1}, theoretically were calculated at 1680 cm^{-1}. While the peaks of –C(O)-O stretching are detected at 1202 cm^{-1}, 1164 cm^{-1} and 1138 cm^{-1} , theoretically were calculated at 1214 cm^{-1}. The aromatic –C-H peak belonging to the -CH_3 group is observed at 3033cm^{-1} (Erdik 2008), were calculated at 3071 cm^{-1} theoretically.

4.3 NMR Results of (E)-4-((p-tolylimino)methyl)phenyl Acrylate Compound

The ^{1}H-NMR spectrum of the compound is shown in Figure 4.3 (Sılku 2014). Using the 6-311++G (d,p) basis set and the DFT/B3LYP technique, calculations were carried out in DMSO solution. The acryloyl group is connected to the structure, as evidenced by the presence of H32 (6.43 ppm), H34 (6.55 ppm), and H35 (6.19 ppm). The study's acquired values are provided in (Table 4.3) alongside the experimental values.

It was found that the H7 and H8 protons moved down to the lower field in relation to the initial compound with the attachment of the acryloyl group. According to the sources, the methyl group's peak in the structure was identified at 2.31 ppm.

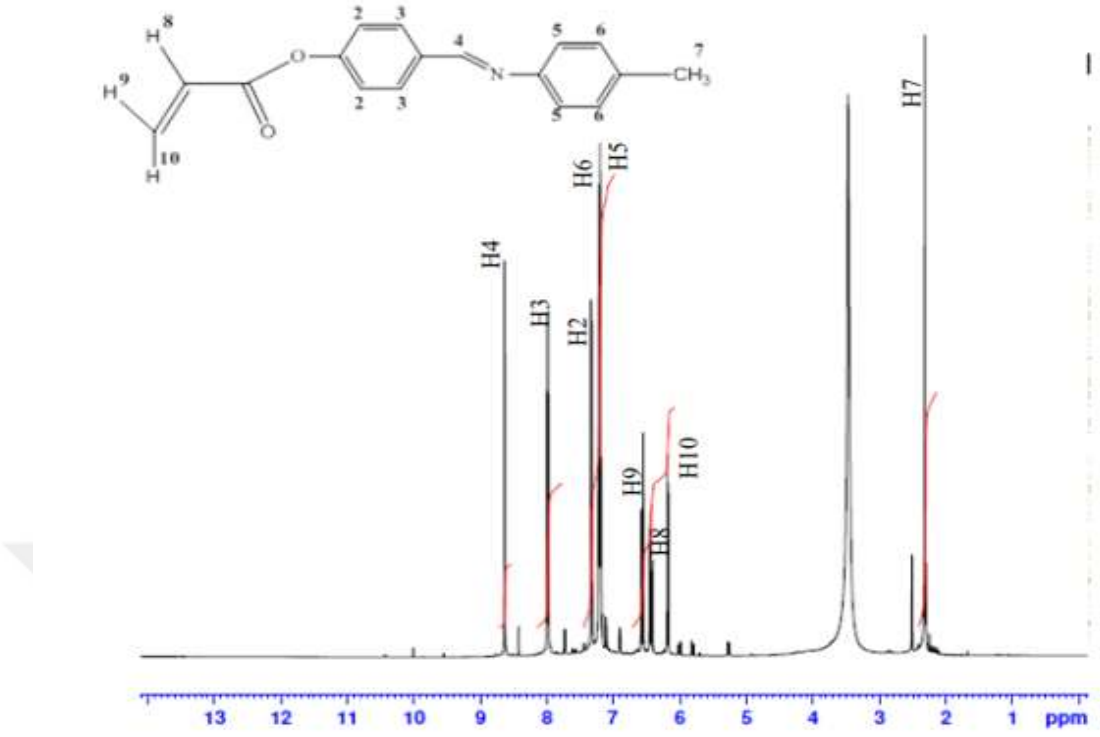

Figure 4.3 ^{1}H-NMR spectrum of (E)-4-((p-tolylimino)methyl)phenyl acrylate compound.

Table 4.3 ^{1}H-NMR and ^{13}C-NMR results of (E)-4-((p-tolylimino)methyl)phenyl acrylate compound

Assignment	**Exp.** (Sılku 2014)	**δcalc.**
C29		162.61
C11		157.73
C6		154.30
C14		150.76
C21		138.44
C33		136.71
C3		134.57
C4		133.09
C31		129.92
C19		129.84
C17		129.30
C2		127.13
C15		125.33
C5		121.88
C1		121.14
C16		116.24
C24		20.38
H8	7.98	8.51
H13		8.48

Table 4.3 (Continued)

H9	7.98	7.70
H10	7.34	7.43
H23	7.21	7.37
H18	7.19	7.34
H22	7.21	7.31
H7	7.34	7.28
H20	7.19	7.06
H35	6.55	6.96
H34	6.19	6.45
H32	6.43	6.26
H25	2.31	2.66
H26	2.31	2.43
H27	2.31	2.19

Transform into using equations given in Refs (Blanco *et al.* 2007, Silva *et al.*2008)

$\delta^{13}C = 175.7–0.963\ \delta^{13}C$ and $\delta^{1}H = 31.0–0.970\ \delta^{1}H$.

4.4 HOMO-LUMO Analyze

The HOMO-LUMO energy gap, also known as the HOMO-LUMO band gap, is the difference in energy between the Highest Occupied Molecular Orbital (HOMO) and the Lowest Unoccupied Molecular Orbital (LUMO) in a molecule or solid substance. The LUMO signifies the lowest energy level that electrons cannot inhabit, whereas the HOMO denotes the highest energy level that an electron may occupy.

Understanding and predicting the electrical properties and behaviour of molecules and materials is strongly reliant on the HOMO-LUMO energy gap.

Understanding and managing the HOMO-LUMO energy gap allows researchers to build and optimize materials for specific electrical, optical, and energy-related applications.

The HOMO and LUMO molecular orbital energies of the investigated molecule were estimated using the DFT/B3LYP technique and the 6-311++G (d,p) basis set, as shown in (Figure 4.4).

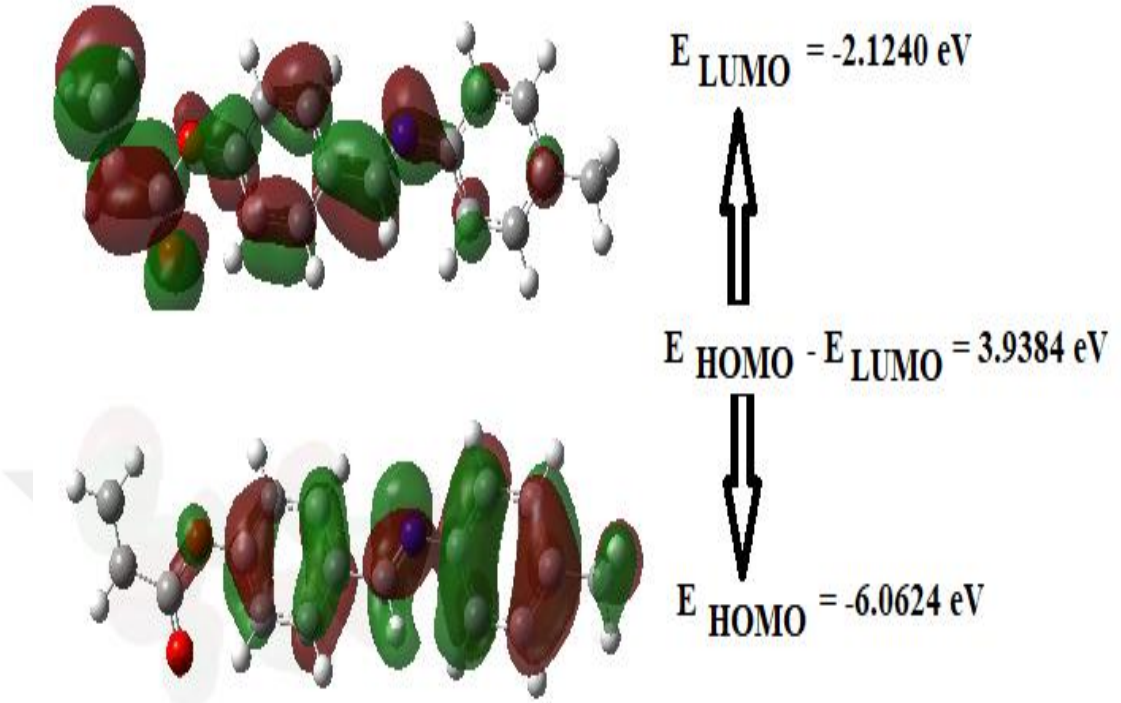

Figure 4.4 Energy levels and the 3D plots of the HOMO and LUMO of the (E)-4-((p-tolylimino)methyl)phenyl acrylate compound

Because there is a 3.93 eV energy difference between HOMO and LUMO, the molecule is thermodynamically robust and stable. The molecule is also conductive.

4.5 Nonlinear Optical (NLO) Properties

Nonlinear optics, which investigates how intense light fields interact with materials, is a recent field within physics with numerous potential applications in both basic science and technology (R.W. Boyd 2002). Nonlinear optical (NLO) effects are studied by examining the atomic response of a dielectric material to the electric fields of an intense light beam.

Static polarizability (α_0), initial static hyperpolarizability (β_{tot}) of structures, and the dipole moment (μ) are all intimately connected to their nonlinear optical (NLO) activity. By The Gaussian 5.0 output, polarizabilities and hyperpolarizabilities have been translated from atomic to electrostatic units.

(α: 1a. u = $0.1482*10^{-24}$esu; β: 1a. u = $8.6393*10^{-33}$esu) (Sundaraganesan *et al*. 2009). The sum of all static dipole moments, μ is defined as shown in this equation:

$$\mu= (\mu_x^2+\mu_y^2+\mu_z^2)^{1/2} \quad (4.1)$$

Below are details of the calculations of static polarizability (αave) and initial static hyperpolarizability (β_{tot}) based on the Gaussian output (Alyar *et al.* 2007):

$$<\alpha> = 1/3\ (\alpha xx + \alpha yy + \alpha zz)$$

$$\beta_{tot} = [(\beta xxx + \beta xyy + \beta xzz)2 + (\beta yyy + \beta yzz + \beta yxx)2 + (\beta zzz + \beta zxx + \beta zyy)2]1/2 \quad (4.2)$$

Urea is viewed as a general reference due to its unique characteristics in the investigation of nonlinear optical properties. The NLO characteristics of the molecules under consideration are assessed by comparing them to urea.

Urea values acquired from DFT/B3LYP/6-311G calculations (d), μ = 1.3732 Debye, α = 3.8312 $Å^3$ and $\beta = 0.37289*10^{-30}$ cm^5/esu (Meganathan *et al*. 2012). Table 4.4 displays the examined the computed electric dipole moment, polarizability, and first-order hyperpolarizability properties of the investigated substance.

Table 4.4 The electric dipole moment μ (D), the mean polarizability <α> and the first hyperpolarizability (βtot) of (E)-4-((p-tolylimino) methyl) phenyl acrylate by DFT/B3LYP/6-311++G (d,p) level of theory

Parameter	**4-((p-tolilimino)methyl)phenyl acrylate**	**Parameter**	**4-((p-tolilimino)methyl)phenyl acrylate**
μ_x	-0.3285	$ß_{xxx}$	-1347.83
μ_y	0.3296	$ß_{xxy}$	-232.97
μ_z	0.5267	$ß_{xyy}$	37.37
μ_{tot}	0.7028	$ß_{yyy}$	19.40
α_{xx}	419.41	$ß_{xxz}$	95.49
α_{xy}	-5.37	$ß_{xyz}$	16.04
α_{yy}	198.40	$ß_{yyz}$	29.65
α_{xz}	-5.65	$ß_{xzz}$	-3.04
α_{yz}	0.88	$ß_{yzz}$	10.19
α_{zz}	129.90	$ß_{zzz}$	42.62
<α> (a.u)	249.23	**β_{tot} (a.u)**	1339.69
<α> (esu)	$36.93*10^{-24}$ esu	**β_{tot} (esu)**	$11573.98*10^{-33}$esu

α: 1a. u = $0.1482*10^{-24}$ esu, β: 1a. u = $8.6393*10^{-33}$esu

The (μ) dipole moment was determined 0.7028 and mean polarizability (α tot) was determined to be 36.93*10-24 esu. The compound's first order hyperpolarizability (βtot) was determined to be 11573.98*10-33esu which is nearly 31 times larger than that of urea.

Based on the results, we reach our conclusion that the topic of this chemical and its derivatives represent a promising field for further research into nonlinear optical properties.

4.6 Molecular Electrostatic Potential (MESP)

The MEP determines whether a proton positioned at any point surrounding the molecule will find the region of the molecule to be attractive or repulsive (Al-Ahmary et al. 2018).

The electronic density of a molecule is the focus of MESP mapping. According to (Yeşilkaynak et al. 2010), this is a great descriptor for comprehending hydrogen bond interactions and pinpointing hydrogen bond positions in electrophilic and nucleophilic processes. As shown in Fig. 4.5, the MEP surfaces were examined using the DFT method (B3LYP) and basis set (6-311++G**) for geometry optimization. The MEP surface's color scheme is as follows: Light blue denotes an area that is somewhat electron-deficient, yellow denotes a region that is slightly electron-rich, green denotes neutral (zero potential), and red denotes an electron-rich, largely negative charge. Blue denotes an electron-deficient, partially positive charge (Politzer and Murray 2002).

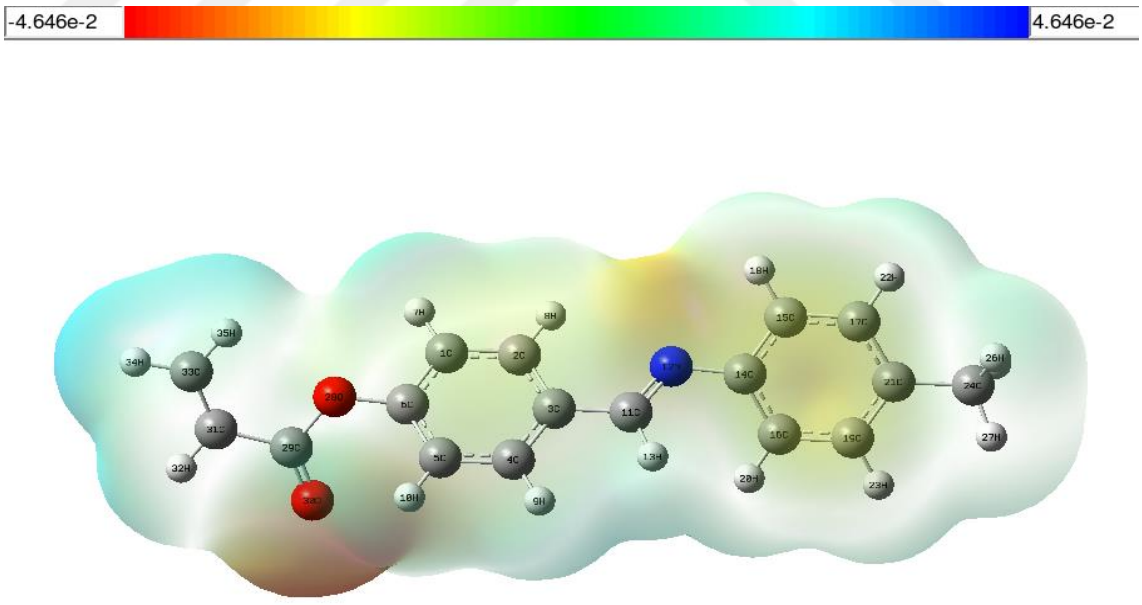

Figure 4.5 MESP map of 4-((p-tolilimino)methyl)phenyl acrylate compound

5. CONCLUSIONS AND RECOMMENDATION

In the study, (E)-4-((p-tolylimino)methyl)phenyl acrylate molecule, First of all, the stable structure with minimum energy of the studied molecule was obtained by DFT method by performing geometry optimization calculation at B3LYP/6-311++G(d,p) level.

Since the molecule studied in the literature have no experimental structural parameters, the theoretically calculated the compound's bond lengths and bond angles were compared to experimental values of similar molecules in the literature. The N-C, C-C and C-O bond lengths were calculated as 1.405, 1.394 and 1.393 Å. It was seen that the calculated results and the experimental values in the literature were compatible with each other. In the FT-IR analysis results obtained with the 6-311++G(d,p) basis set we used with the DFT/B3LYP method, it is seen that the value of 3071 cm-1 calculated for the –C-H stretching vibration almost coincide with the value of similar molecule groups (Erdik 2008).

In addition, the absence of virtual vibration frequency values (negative number) indicates that the molecule is optimized with correct calculation methods and has a stable structure. After examining the vibration frequencies of the studied molecule, 1H-NMR and 13C-NMR chemical shift values were calculated. The HOMO and LUMO energies of the (E)-4-((p-tolylimino)methyl)phenyl acrylate molecule were calculated by the DFT method at the B3LYP/6-311++G(d,p) level. The obtained HOMO and LUMO energy difference was found to be 3.9384 eV. The nonlinear optical properties and molecular potential energy surface map of the studied compound were calculated using the same method and basis set. As a result of calculation, the compound was found to have a hyperpolarizability of $11573.98*10^{-33}$esu. This value indicates that the hyperpolarizability of the compound is approximately 31 times larger than that of urea. Therefore, it can be said that the compound exhibits nonlinear optical properties.

On the molecular potential energy surface, the red regions indicate electron-rich regions, and the gray and blue regions indicate electron-poor regions. In this thesis, all calculations were performed with Gaussian 09 and Gauss View 5.0 package program.

REFERENCES

Al-Ahmary, K. M., Mekheimer, R. A., Al-Enezi, M. S., Hamada, N. M., and Habeeb, M. M. (2018). Synthesis, spectrophotometric characterization and DFT computational study of a novel quinoline derivative, 2-amino-4-(2, 4, 6-trinitrophenylamino)-quinoline-3-carbonitrile. Journal of Molecular Liquids, 249, 501-510.

Al-Hamdani, A. H., Ibrahim, S. I., Jawad, R. S., Nader, R., Adnan, D., and Jabir, M. (2016). Non-linear properties measurement for liquid solution of α-chlorophyll dissolved in acetone. International Journal of Computation and Applied Sciences IJOCAAS, 1(2), 28-36.

Al-kaissy, A. H. (2011) "Nonlinear Optical Properties of Epoxy/Alumina Nanocomposites ", M.Sc. thesis, University of Baghdad Institute of Laser for Postgraduate Studies.

Al-Sarraji, I. K. (2014) "Optical Properties of Prepared Nanostructure Palladium", M.Sc. thesis, University of Baghdad Institute of Laser for Postgraduate Studies.
in Communication Electronics, Wiley, Chapter 4.

Alyar, H., Alyar, S., Ünal, A., Özbek, N., Şahin, E., & Karacan, N. (2012). Synthesis, characterization and antimicrobial activity of m-toluenesulfonamide, N, N′-1, 2-ethanediylbis (mtsen) and [Cu (II)(phenanthroline) 2] mtsen complex. Journal of Molecular Structure, 1028, 116-125.

Alyar, H., Kantarci, Z., Bahat, M., & Kasap, E. R. G. Ü. N. (2007). Investigation of torsional barriers and nonlinear optical (NLO) properties of phenyltriazines. Journal of molecular structure, 834, 516-520.

Alyar, H., Ünal, A., Özbek, N., Alyar, S., & Karacan, N. (2012). Conformational analysis, vibrational and NMR spectroscopic study of the methanesulfonamide-N, N′-1, 2-ethanediylbis. Spectrochimica Acta Part A: Molecular and Biomolecular Spectroscopy, 91, 39-47.

Alyar, S., Adem, Ş. (2014). Synthesis, characterization, antimicrobial activity and carbonic anhydrase enzyme inhibitor effects of salicilaldehyde-N-methyl p-toluenesulfonylhydrazone and its Palladium (II), Cobalt (II)

complexes. Spectrochimica Acta Part A: Molecular and Biomolecular Spectroscopy, 131, 294-302.

Ashraf M., Wajid A., Mahmood K., Maah M., Yusoff I. 2011."Spectral Investigation of the Activities of Amino Substituted Bases", Orient. J. Chem., 27: 363–372.

Aydınlı Esen A. 2006. "Bazı Schiff Bazlarının Antimikrobiyal Etkileri", Yüksek Lisans, Ankara Üniversitesi Fen Bilimleri Enstitüsü.

Baden Fuller, A. J. (1979) Microwaves, Pergamon, 2nd edn, Chapter 3.

Benson, F. A. (Ed.). (1969). Millimetre and submillimetre waves. Iliffe Books Limited.

Blanco, F., Alkorta, I., & Elguero, J. (2007). Statistical analysis of 13C and 15N NMR chemical shifts from GIAO/B3LYP/6-311++ G** calculated absolute shieldings. Magnetic Resonance in Chemistry, 45(9), 797-800.

Bransden, B. H., and Joachain, C. J. (2003). Physics of atoms and molecules. Pearson Education India.

C. J. Cramer. (2004) " Essentials of Computational Chemistry: Theories and Models", 2nd edition, John Wiley & Sons Ltd., Chichester, England.

Cheng, O.K. (1990) Field and Wave Electromagnetics, Addison-Wesley, 2nd edn.

Clementi, E., André, J. M., and McCammon, J. A. (Eds.). (2012). Theory and Applications in Computational Chemistry: The First Decade of the Second Millennium. American Institute of Physics, ISBN 978-0-7354-1057-2, 275 page.

Coates, J. (2006). Interpretation of infrared spectra, a practical approach. Encycl. Anal. Chem.

Collin, R. E. (1966) Foundationsfor Microwave Engineering, McGrawHill.

Crawford, T. D., Sherrill, C. D., Valeev, E. F., Fermann, J. T., King, R. A., Leininger, M. L., ... and Allen, W. D. (2007). PSI3: an open-source ab initio electronic structure package. Journal of computational chemistry, 28(9), 1610-1616.

Cresswell, A. J., Sanderson, D. C., and Yamaguchi, K. (2018). Assessment of the calibration of gamma spectrometry systems in forest environments. Journal of Environmental Radioactivity, 181, 70-77.

Cullen, A. L. (1965). Electronics Division: summary of Chairman's address. Waveguides. Electronics and Power, 11, 382.

Dewar, M. J. S. (1969). Molecular orbital theory of organic chemistry.; see also Murrell, J. N., and Harget, A. J. (1972). Semi-empirical self-consistent-field molecular orbital theory of molecules., Wiley-Interscience, London.

Dirisio, R. J., Armstrong J. E., Frank M. A., Lake W. R., McNamara W. R. 2017. "Cobalt Schiff-base complexes for electrocatalytic hydrogen generation", Dalton Trans., 46: 10418-10425.

Emregül K. C., Düzgün E., Atakol O. 2006. "The application of some polydentate Schiff base compounds containing aminic nitrogens as corrosion inhibitors for mild steel in acidic media", Corr. Sci., 48: 3243-3260.

Erdik, E. (2008). Organik kimyada spektroskopik yöntemler, 5. Baskı. Gazi Büro Kitabevi.

Fitts, D. D. (1999). Principles of quantum mechanics: as applied to chemistry and chemical physics. Cambridge University Press.

Fitts, D. D. (2002). Principles of quantum mechanics: as applied to chemistry and chemical physics. Cambridge University Press.

Fock, V. (1930). Näherungsmethode zur Lösung des quantenmechanischen Mehrkörperproblems. Zeitschrift für Physik, 61(1-2), 126-148.

García, R., and Báez, A. P. (2012). Atomic absorption spectrometry (AAS). Atomic absorption spectroscopy, 1, 1-13.

Gilmore, G. (2008). Practical gamma-ray spectroscopy. 2nd ed. John Wiley & Sons Ltd.

Golcu A., Tümer M., Demirelli H., Wheatley R.2005. "Cd(II) and Cu(II) complexes of polydentate Schiff base ligands: synthesis, characterization, properties and biological activity", Inorg. Chim. Acta, 358: 1785-1797.

Hehre, W. J. (2003). A guide to molecular mechanics and quantum chemical calculations (Vol. 2). Irvine, CA: Wavefunction.

Hund, F. (1927). On the interpretation of molecular spectra I. Zeitschrift für Physik, 40, 742.

Jaber, W. 2015. A Study of Optical Properties of Acridine Dye and Alumina Nanoparticles Doped in PMMA Polymer, M.Sc. thesis, University of Babylon.

Jensen, F. "Introduction to Computational Chemistry", 2nd edition, John Wiley & Sons Ltd., Chi.

Kaupp, M. (2001). Buchbesprechung: A Chemist's Guide to Density Functional Theory. Von Wolfram Koch und Max C. Holthausen. Angewandte Chemie, 113(5), 989-990.

Kaxiras, E. (2003). "Atomic and Electronic Structure of Solid", Cambridge University Press, New York, USA.

Khalaf, R. (2013). Manshad. Studing of Nonlinear Optical Properties for Organic Dye (Doctoral dissertation, thesis, University of Basrah).

Khan, H. M., Chaudhry, Z. S., Ismail, M., and Khan, K. (2010). Assessment of radionuclides, trace metals and radionuclide transfer from soil to food of Jhangar Valley (Pakistan) using gamma-ray spectrometry. Water, Air, & Soil Pollution, 213, 353-362.

Khopkar, S. M. (1998). Basic concepts of analytical chemistry. New Age International.

Kiran, P. P., Rao, S. V., Ferrari, M., Krishna, B. M., Sekhar, H., Alee, S., and Rao, D. N. (2010). Enhanced optical limiting performance through nonlinear scattering in nanoparticles of CdS, co-doped Ag-Cu, and BSO. Nonlinear Opt Quantum Opt, 40, 223-234.

Kohanoff, J., and Gidopoulos, N. I. (2003). Density functional theory: basics, new trends and applications. Handbook of molecular physics and quantum chemistry, 2(Part 5), 532-568.

Kudelski, A. (2008). Analytical applications of Raman spectroscopy. Talanta, 76(1), 1-8.

Kudelski, A. (2009). Raman spectroscopy of surfaces. Surface Science, 603(10), 1328-1334.

Kuhn, S. (1946). Calculation of attenuation in wave guides. Journal of the Institution of Electrical Engineers- 3 (IIIA), 663-78.

Kwon, J. (2012). Applications of semi-empirical quantum mechanical calculations to simple molecular systems (Doctoral dissertation).

Lakowicz, J.R. (2006) Principles of Fluorescence Spectroscopy, 3rd ed., Kluwer Academic/Plenum Publishers, New York.

Lide, D. (2012) " Chemistry and Physics" Preprint of CRC Handbook, 92 Edition, Boca Raton, FL.: CRC Press/Taylor and Francis, 6–232.

Long, D. A. (1977). Raman spectroscopy. New York, 1-12.

Lonsdale, R., Harvey, J. N., and Mulholland, A. J. (2012). A practical guide to modelling enzyme-catalysed reactions. Chemical Society Reviews, 41, 3025-3038.

Mahdi, Z. F. (2010). Improvement of nonlinear optical properties for mixture laser dyes doped PMMA. Iraqi J. Laser, 9(2), 9-14.

Marenich, A. V., Ho, J., Coote, M. L., Cramer, C. J., and Truhlar, D. G. (2014). Computational electrochemistry: prediction of liquid-phase reduction potentials. Physical Chemistry Chemical Physics, 16(29), 15068-15106.

Meganathan, C., Sebastian, S., Sivanesan, I., Lee, K. W., Jeong, B. R., Oturak, H., ... & Sundaraganesan, N. (2012). Structural, vibrational (FT-IR and FT-Raman) and UV–Vis spectral analysis of 1-phenyl-3-(1, 2, 3-thiadiazol-5-yl) urea by DFT method. Spectrochimica Acta Part A: Molecular and Biomolecular Spectroscopy, 95, 331-340.

Meyer, E. R. N. S. T. (1992). Atomic force microscopy. Progress in surface science, 41, 3-49.

Mueller, M. P. (2007). Fundamentals of quantum chemistry: molecular spectroscopy and modern electronic structure computations. Springer Science & Business Media.

Muncheryan, H. M. (1983). Principles and practice of laser technology.

Neumann, J. v. and Wigner, E. P. Z. (1929), Phys. 30. 467.

of Electromagnetic Waves, Cambridge University Press, Chapter 2.

Ojeda, J. J., and Dittrich, M. (2012). Fourier transform infrared spectroscopy for molecular analysis of microbial cells. Microbial Systems Biology: Methods and Protocols, 187-211.

Ozaslan M., Karagöz I. D., Kılıç I. H., Güldür M. E. 2011. “Ehrlich ascites carcinoma”, Afr. J. Biotechnol., 10: 2375-2378.

Pfeiffer P., Breith E., Lubbe E., Tsumaki T. 1933. “Tricyclische Orthokondenzierte Nebenvolenzringe”, Annalen Der Chemie, 503: 84-127.

Politzer, P., and Murray, J. S. (2002). The fundamental nature and role of the electrostatic potential in atoms and molecules. Theoretical Chemistry Accounts, 108, 134-142.

Pople, J. A., and Beveridge, D. L. (1970). Approximate molecular orbital Theory', McGraw-Hill, New York, 75.

Pople, J. A., and Segal, G. A. (1966). Approximate self-consistent molecular orbital theory. III. CNDO results for AB2 and AB3 systems. The Journal of Chemical Physics, 44, 3289.

R.W. Boyd, Nonlinear Optics (Academic press, 2002).

Radhi, S. F. (2012). Nonlinear responses and optical limiting behavior of 2-Chloro-5-nitroanisole dye under CW laser illumination. journal of kerbala university, 10(4), 181-186.

Raman, C. V., and Krishnan, K. S. (1928). Polarisation of scattered light-quanta. Nature, 122, 169.

Ramo, S., Whinnery, J. R. and Van Duzer, T. (1967) Fields and Waves.

Redshaw, C. 2017. "Use of Metal Catalysts Bearing Schiff Base Macrocycles for the Ring Opening Polymerization (ROP) of Cyclic Esters", Catalysts, 7(5): 165-176.

Rehman W., Baloch M. K., Muhammad B., Badshah A., Khan K. M. 2004. "Characteristic spectral studies and in vitro antifungal activity of some Schiff bases and their organotin (IV) complexes", Chin. Sci. Bull., 49: 119-122.

Rekha, R. K., and Ramalingam, A. (2009). Optical nonlinear properties and optical limiting effect of metanil yellow. Am. J. Eng. Appl. Sci, 2(2), 285-291.

Roberts, D. W., Schultz, T. W., Api, A. M. 2017. "Skin Sensitization QMM for HRIPT NOEL Data: Aldehyde Schiff-Base Domain", Chem. Res. Toxicol., 30(6): 1309-1316.

Rogers, D. W. (2003). Computational Chemistry using the PC. John Wiley & Sons, ISBN 0-471-42800-0, 343 page.

Rouze, G. S., Morgan, C. L. S., & McBratney, A. B. (2017). Understanding the utility of aerial gamma radiometrics for mapping soil properties through proximal gamma surveys. Geoderma, 289, 185-195.

Sander, K. F. and Reed, G. A. L. (1978) Transmission and Propagation

Schiff, H. 1869. "Untersuchungen Uber Salicin Derivate", Eur. J. Org. Chem., 150; 193-200.

Seçkin T., Köytepe S., Demir S., Özdemir İ., Çetinkaya B.2003. "Novel type of metal-containing polyimides for the heck and Suzuki-Miyaura cross-coupling reactions as highly active catalysts", J. Inorg. Organomet P., 13(4): 223-235.

Serin, S., Gök, Y. 1988. "Hidroksi Schiff Bazı Metal Komplekslerinin Tekstil Boyamacılığında Kullanabilirliğinin İncelenmesi", T. Kimya D.C., 12: 325-331.

Sharaby, C. M., Amine, M. F., Hamed, A. A. 2017. "Synthesis, structure characterization and biological activity of selected metal complexes of sulfonamide Schiff base as a

primary ligand and some mixed ligand complexes with glycine as a secondary ligand", J. Mol. Struct., 1134: 208-216.

Sholl, D., and Steckel, J. A. (2011). Density functional theory: a practical introduction. John Wiley & Sons.

Sılku, P. (2014). Density functional theory: a practical introduction Bazı yeni imin bileşiklerinin eldesi, spektroskopik özelliklerinin belirlenmesi ve inhibitör özelliklerinin incelenmesi. MSc. Thesis, Hitit University, 116 page, Çorum.

Silva da C., Silva da D., Modolo L., Alves R.2011."Schiff bases: A short review of their antimicrobial activities", J. Ad. Res., 2: 1-8.

Silva, A. M., Sousa, R. M., Jimeno, M. L., Blanco, F., Alkorta, I., & Elguero, J. (2008). Experimental measurements and theoretical calculations of the chemical shifts and coupling constants of three azines (benzalazine, acetophenoneazine and cinnamaldazine). Magnetic Resonance in Chemistry, 46(9), 859-864.

Skoog D.A. and Leary J.J. (1992) Principles of instrumental analysis. Saunders College, Philadelphia.

Skoog, D. A., West, D. M., Holler, F. J., and Crouch, S. R. (2013). Fundamentals of analytical chemistry. Cengage learning.

Staniforth, J. A. (1972). Microwave Transmission. English Universities Press.

Sundaraganesan, N., Kavitha, E., Sebastian, S., Cornard, J. P., & Martel, M. (2009). Experimental FTIR, FT-IR (gas phase), FT-Raman and NMR spectra, hyperpolarizability studies and DFT calculations of 3, 5-dimethylpyrazole. Spectrochimica Acta Part A: Molecular and Biomolecular Spectroscopy, 74(3), 788-797.

Upadhyay, K. K., Kumar, A., Upadhyay, S., Mishra, P. C. 2008. "Synthesis, characterization, structural optimization using density functional theory and superoxide ion scavenging activity of some Schiff bases", J. Mol. Struct., 873: 5-16.

Valone, S. M. (2010). Quantal Density Functional Theory II. Approximation Methods and Applications, 132 (32), 11387–11388.

Van der Kamp, M. W., and Mulholland, A. J. (2013). Combined quantum mechanics/molecular mechanics (QM/MM) methods in computational enzymology. Biochemistry, 52, 2708-2728.

Yesilkaynak, T., Binzet, G., Emen, F. M., Flörke, U., Külcü, N., & Arslan, H. (2010). Theoretical and experimental studies on N-(6-methylpyridin-2-yl-carbamothioyl) biphenyl-4-carboxamide. European Journal of Chemistry, 1(1), 1-5.

Yong, D. C. (2001). Using existing basis sets. Computational Chemistry: A Practical Guide for Applying Techniques to Real-World Problems; John Wiley & Sons, Inc.: New York, NY, USA, 10, 78-98.

William, M.S.(2003) "Laser Material Processing", Springer, Verlag London,3th Edition.

CURRICULUM VITAE

Personal Information

Name and Surname : ABDULRAHMAN JAMAL HASHIM AL-DHUWAIB

Education

Undergraduate	University of Anbar College of Educatıon for Pure Sciences Department of Physics	2010-2014
MSc	Çankırı Karatekin University Graduate School of Natural and Applied Sciences Department of Physics	2020-2023

Work Experience

During my postgraduate studies, I published my first article in the International Journal of Research in Engineering and Sciences in 2023.